Drew University

College of Liberal Arts

The Synthesis and Analysis of Triosmium Carbonyl Clusters with Potential Biological Activity

A Thesis in Chemistry

By

Paxtan Perry

Examining Committee:

Mary-Ann Pearsall, Thesis Advisor

Chemistry

Adam Cassano, Member

Chemistry

Jim Supplee, Member

Physics

May 2022

Table of Contents

1. Abstract
2. Introduction
    a. General Chemistry of Osmium Carbonyl Clusters
        i. Introduction of $Os_3(CO)_{10}(\mu\text{-}OEt)_2$
        ii. The Reactivity of 3 Os-Os Bonds versus 2 Os-Os Bonds with Bridging Ligands
            1. Reactions of Osmium Carbonyl Complexes with $P(OMe)_3$
            2. Reactions of Osmium Carbonyl Complexes with MeCN
    b. Research Focus
    c. Biological Applications of Transition Metal Complexes
        i. Osmium Carbonyl Complexes
        ii. Dirhodium Complexes
        iii. Proposed biological investigation of $Os_3(CO)_{10-x}(\mu\text{-}OEt)_2(MeCN)_x$
3. Methods
    a. FT-Infrared Spectroscopy
    b. Thin Layer Chromatography
    c. Nuclear Magnetic Resonance
    d. Synthesis Techniques
4. Experimental
    a. Experimental synthesis of triosmium decacarbonylbisethoxide $Os_3(CO)_{10}(\mu\text{-}OEt)_2$
    b. Experimental synthesis attempt of $Os_3(CO)_8(\mu\text{-}OEt)_2(NCMe)_2$

c. Experimental synthesis of $Os_3(CO)_9(\mu\text{-}OEt)(MeCN)$ with $P(OMe)_3$

d. Experimental synthesis of $Os_3(CO)_9(\mu\text{-}OEt)(MeCN)$ with PPh_3

5. Results and Discussion

    i. Reaction of $Os_3(CO)_{10}(\mu\text{-}OEt)_2$ in acetonitrile

    ii. Reaction of $Os_3(CO)_{10\text{-}x}(\mu\text{-}OEt)_2(MeCN)_x$ with $P(OMe)_3$

    iii. Reaction of $Os_3(CO)_{10\text{-}x}(\mu\text{-}OEt)_2(MeCN)_x$ with PPh_3

6. Conclusion and Future Directions

7. Discovery and Synthetic Routes of $Os_3(CO)_{10}(\mu\text{-}OEt)_2$ – A Review

    a. Discovery as a biproduct

    b. Schlecht – synthesis of dihalo-bridged clusters from linear Os-dihalide complex

    c. Shah – synthesis of bisethoxide from linear Os-dichloride intermediate

    d. Portero – synthesis of bisethoxide from linear Os-dibromide and Os-diiodide intermediates

    e. Rivero – synthesis of bisethoxide from dihalo-bridged complexes

        i. Testing alumina to balance equilibrium

    f. Sommerhalter – synthesis of bisethoxide of dihalo-bridged complexes with alumina in initial reaction mixture

    g. Utilization of microwave synthesis; current synthetic pathway

    h. Reactions of Bisethoxide

8. Works Cited

1. Abstract

Several triosmium carbonyl clusters demonstrate biological activity in published literature[1]. These various complexes possess labile ligands, which have been shown to be responsible for potential biological activity. The biological reactivity of triosmium decacarbonyl bisethoxide, (bisethoxide, ($Os_3(CO)_{10}(\mu\text{-}OEt)_2$), and synthetic derivatives are not yet known, but are predicted to be similar to other biologically active triosmium complexes based on their similarity in chemical reactivity and structure. In this research, the complexes $Os_3(CO)_8(\mu\text{-}OEt)_2(NCMe)_2$ and $Os_3(CO)_9(\mu\text{-}OEt)_2(NCMe)$ have been synthesized where acetonitrile is a labile ligand. Reaction progress was monitored through Infrared Spectroscopy (IR) and Thin Layer Chromatography (TLC); while IR, TLC, and Proton Nuclear Magnetic Resonance spectroscopy (^1H NMR) were used for product confirmation. IR and ^1H NMR analysis deduced the complex $Os_3(CO)_9(\mu\text{-}OEt)_2(NCMe)$ is formed at room temperature, while it is proposed through IR analysis that $Os_3(CO)_8(\mu\text{-}OEt)_2(NCMe)_2$ is formed at high temperatures. In order to be biologically active, osmium carbonyl complexes must be soluble in polar solvents, particularly water, so compounds synthesized in this project were tested for solubility in acetonitrile, ethanol, and water. $Os_3(CO)_{10}(\mu\text{-}OEt)_2$ was found to be soluble in ethanol and not easily soluble in acetonitrile and water. Future evaluation of the solubility of $Os_3(CO)_9(\mu\text{-}OEt)_2(NCMe)$ is needed, as the complex decomposed within 36 hours of production (confirmed by ^1H NMR). The final chapter serves as a review of synthetic approaches to synthesize $Os_3(CO)_{10}(\mu\text{-}OEt)_2$.

2. Introduction

a. General Chemistry of Osmium Carbonyl Clusters

i. Introduction of $Os_3(CO)_{10}(\mu\text{-}OEt)_2$

Triosmium dodecacarbonyl $Os_3(CO)_{12}$, the parent molecule for osmium carbonyl cluster research, contains three osmium-osmium metal bonds and twelve carbonyl ligands. By replacing one of the three metal-metal bonds in the triosmium dodecacarbonyl complex with two bridging ethoxides ligands ($(\mu\text{-}OEt)_2$, where bridging ligands are denoted by the symbol μ), it forms a triosmium complex with only two metal-metal bonds (Figure I.1). This complex with two metal-metal bonds and bridging ethoxide ligands is our starting material triosmium decacarbonylbisethoxide, $Os_3(CO)_{10}(\mu\text{-}OEt)_2$, referred to as "bisethoxide." Because the bridging ethoxides ligands are replacing the third Os-Os metal bond, our work is to understand how this affects the reactivity of the osmium complex.

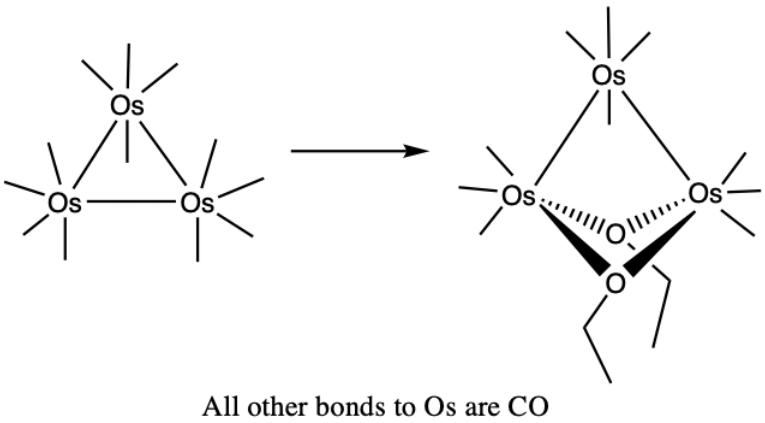

Figure I.1. Structural comparison of triosmium dodecacarbonyl (left) and bisethoxide (right).

Bisethoxide, $Os_3(CO)_{10}(\mu\text{-}OEt)_2$, is shown in three different representations below in Figures I.2 and I.3. To truly understand the reactivity of the molecule, it is important to

understand its structure and molecular components. In Figure I.2, there are two representations of the spatial configuration of bisethoxide, where the two Os-Os metal bonds are emphasized in blue and the bridging ethoxide groups are emphasized in red (osmium = blue, carbon = gray, oxygen = red). These structures show the bridging ethoxide groups that replace the third osmium-osmium bond found in triosmium dodecacarbonyl; the electron counts for this transformation can be seen in Figure I.4.

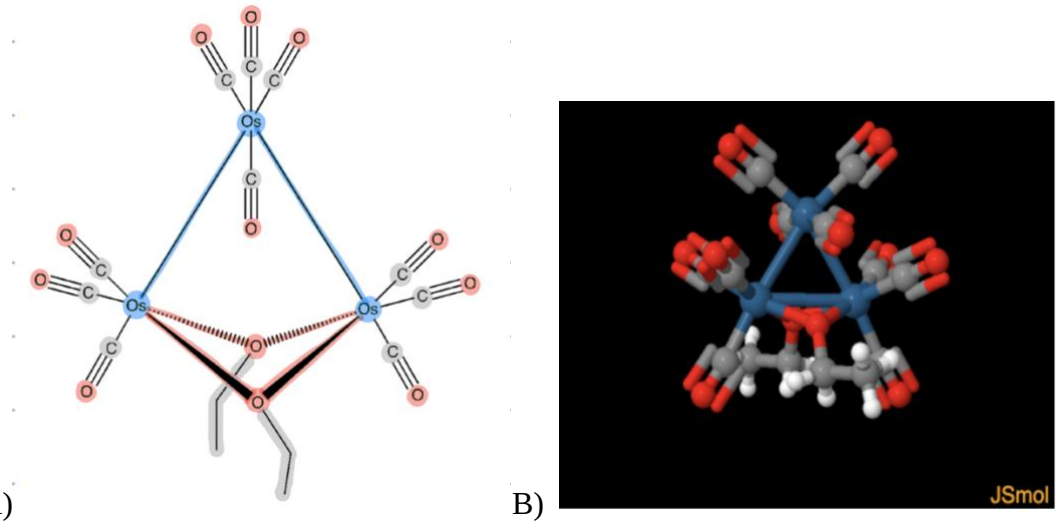

Figure I.2. (A) Representation of bisethoxide; (B) sketch of bisethoxide[2].

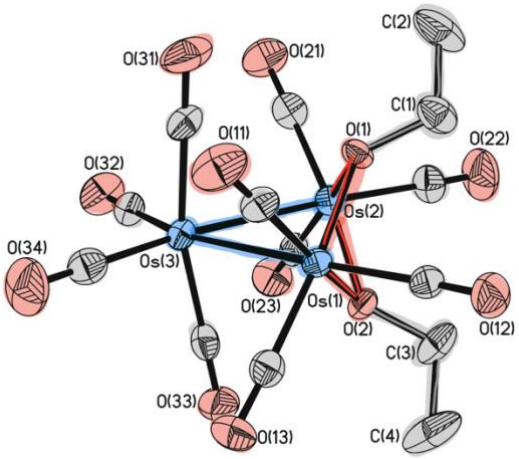

Figure I.3. Crystal structure of bisethoxide, color coded to emphasize bonds[2].

Figure I.3 is an X-ray crystal structure of bisethoxide[2]. The ethoxides replace the third Os-Os bond that we see in triosmium dodecacarbonyl. The crystal structure shows that the ethoxides are facing away from each other, most likely because of steric effects. The osmium center molecules have the smallest thermal ellipsoids because they possess a more defined spatial position and are contained. The bigger thermal ellipsoids shown are the oxygens of the carbonyl ligands and the carbons in the ethoxides show the uncertainty of their location, as these can move and rotate much more freely than can the carbon of the carbonyl ligand or the oxygen of the ethoxide.

It is possible to replace the third osmium-osmium bond found in triosmium dodecacarbonyl with ethoxide groups because the complex still satisfies the 18-electron rule (Figure I.4). The 18-electron rule is used in inorganic chemistry for transition metal complexes and proposes that for each metal atom, there are 18 electrons (e^-) that surround that metal. The $18e^-$ rule can also predict the number of metal-metal bonds in a transition metal cluster. Because there are three osmiums in this cluster, there is a total of $54e^-$ distributed to both clusters ($18e^-$ per each metal); where Os_3CO_{12} has $48e^-$ assigned and bisethoxide has $50e^-$ assigned. The remaining

electrons can be assigned to the number of metal bonds ($2e^-$ per metal-metal bond), so $Os_3(CO)_{12}$ possesses three Os-Os bonds and bisethoxide has two.

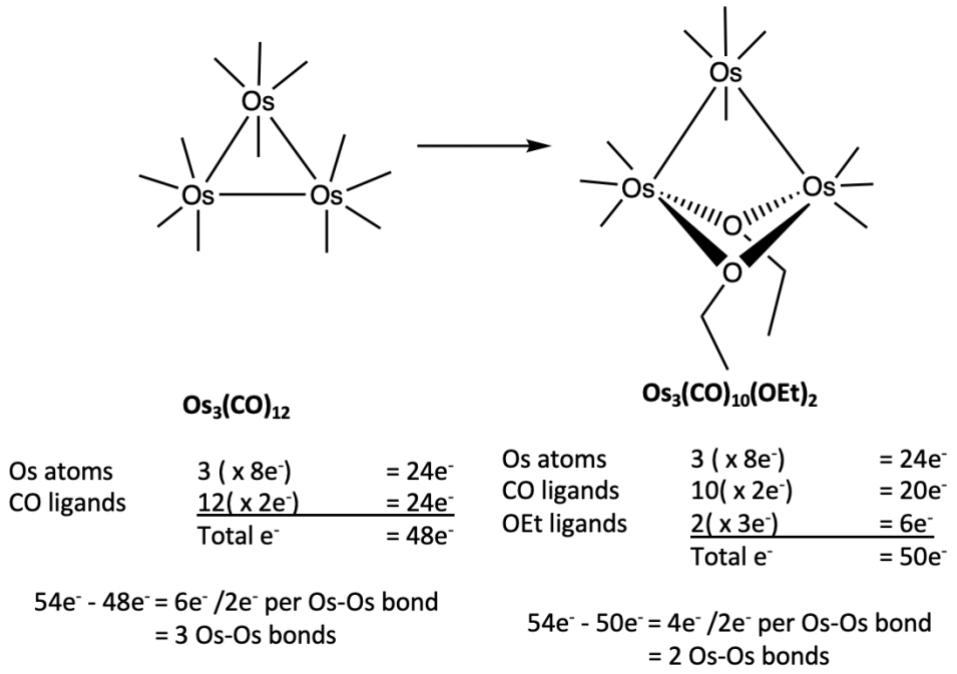

Figure I.4. 18-Electron counts for $Os_3(CO)_{12}$ and $Os_3(CO)_{10}(\mu\text{-}OEt)_2$ used to predict the number of osmium-osmium bonds in each cluster. All other bonds to osmium are CO ligands.

ii. The Reactivity of 3 Os-Os Bonds versus 2 Os-Os Bonds with Bridging Ligands

The complexes triosmium dodecacarbonyl, $Os_3(CO)_{12}$, and bisethoxide, $Os_3(CO)_{10}(\mu\text{-}OEt)_2$, have distinctly different reactivities. By replacing one of the Os-Os bonds of $Os_3(CO)_{12}$ bridged complex, the reactivity of the complex increases by creating another type of reactive site at the bridging ligand position (Figure I.5).

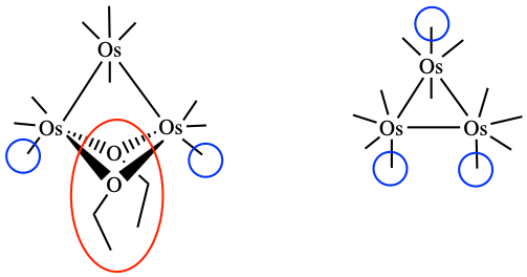

Figure I.5. Reactive sites of $Os_3(CO)_{10}(\mu\text{-}OEt)_2$ (left) and $Os_3(CO)_{12}$ (right). Highlighted in blue are the reactive sites where a carbonyl will be replaced; highlighted in red is the bridging ligand position specifically of bisethoxide where ligands can also be substituted. All bonds to osmium are CO ligands.

For the non-bridged cluster, the only reaction pathway is the replacement of a carbonyl ligand attached to an Os center. This is not easy, as the cluster is considered to be kinetically inert due to its high activation energy arising from the strong Os-C bond – but can occur at any one of the three osmium centers. For the bridged cluster, ligands can also substitute at the bridged position, while still having the ability to replace the attached carbonyl ligands trans to the Os-Os bond; thus having two different reactive sites.

The bridged cluster $Os_3(CO)_{10}(\mu\text{-}OEt)_2$ has one less M-M bond due to the presence of the bridging ethoxide ligands. Complexes with bridging ligands are proven to have higher reactivity as there is more available electron density donation from the osmium cores that possesses CO ligands due to bridged ligands attached to them. The carbonyl ligands trans to the Os-Os bond have been found to be the most labile due to the presence of the bridging center ligands. Therefore the replacement of these carbonyl ligands creates a reactive site in addition to the bridged ligand site (Figure I.5). Thus, the complex possessing these bridged ethoxide ligands enhance the overall reactivity of the complex and transform the complex from being inert (in $Os_3(CO)_{12}$) to labile (in $Os_3(CO)_{10}(\mu\text{-}OEt)_2$.

1. Reactions of Osmium Carbonyl Complexes with $P(OMe)_3$

The different reactivities of these clusters can be illustrated by comparing syntheses with the same ligand. In this work, one ligand of focus is trimethylphosphite, $P(OMe)_3$.

When $Os_3(CO)_{12}$ with $P(OMe)_3$ in a decane solvent is heated to a controlled temperature of 92ºC, it is observed that three products are formed; $Os_3(CO)_9(P(OMe)_3)_3$, $Os_3(CO)_{10}(P(OMe)_3)_2$, and $Os_3(CO)_{11}(P(OMe)_3)$, where the trimethylphosphite ligand substitutes in the trans position (Figure I.6)[3].

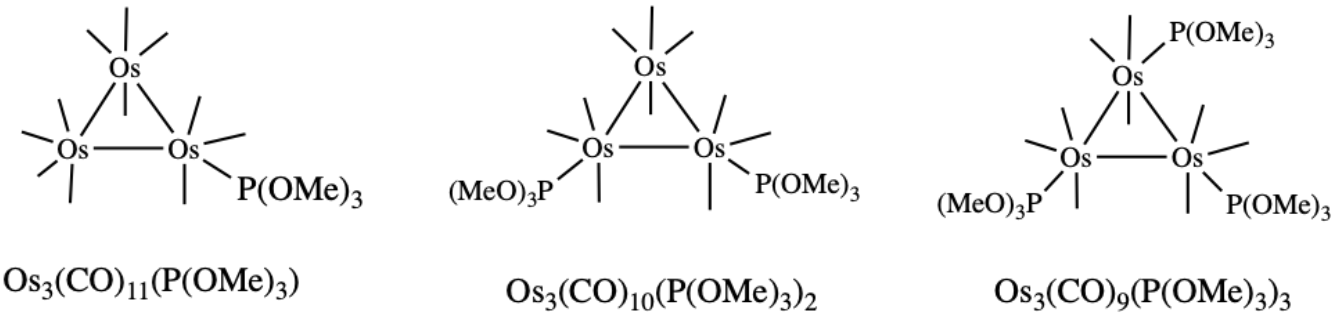

Figure I.6. Possible products that form when $Os_3(CO)_{12}$ is reacted with $P(OMe)_3$ at high temperatures. These substitutional patterns are only seen with $Os_3(CO)_{12}$.

When $Os_3(CO)_{10}(\mu\text{-}OEt)_2$ is heated to 69ºC with $P(OMe)_3$, the disubstituted product $Os_3(CO)_8(\mu\text{-}OEt)_2(P(OMe)_3)_2$ is formed[4]. The $P(OMe)_3$ ligands replaced the carbonyl ligands in the trans to Os-Os bond position (Figure I.7). When $Os_3(CO)_{10}(\mu\text{-}OEt)_2$ is reacted with $P(OMe)_3$ at room temperature however, no substitution occurs.

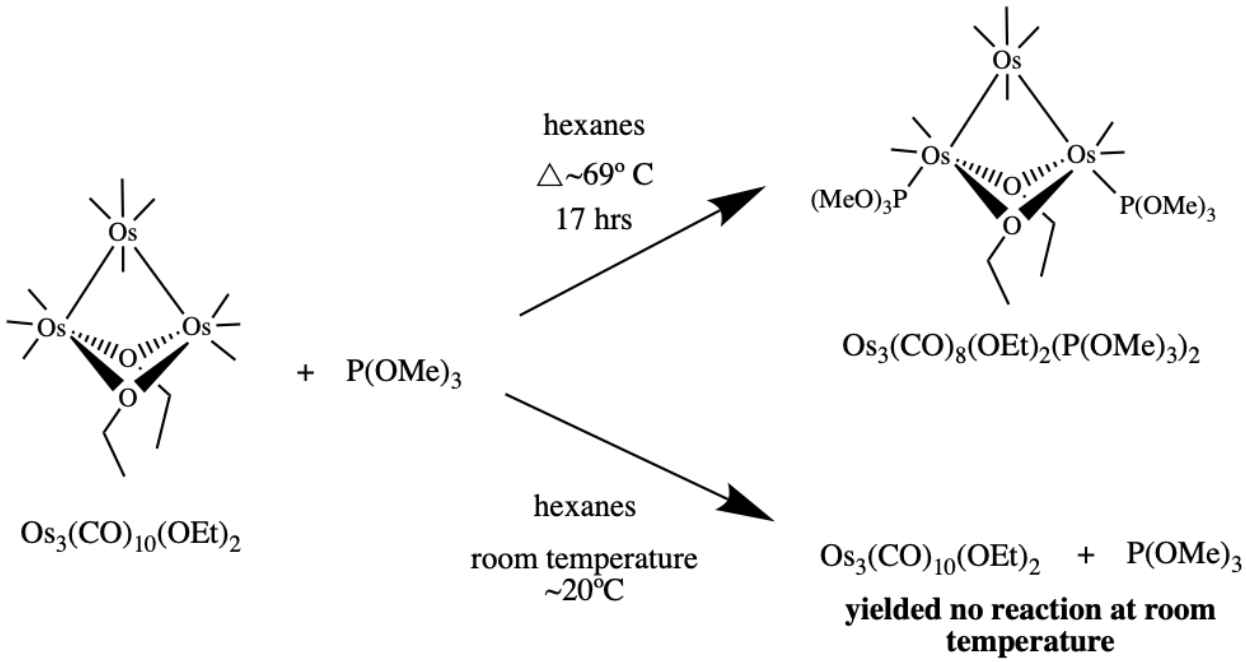

Figure I.7. Reaction scheme of bisethoxide heated with $P(OMe)_3$, and with $P(OMe)_3$ at room temperature.

The substitution position of the $P(OMe)_3$ ligand in both $Os_3(CO)_{10}(P(OMe)_3)_2$) and $Os_3(CO)_{10}(\mu\text{-}OEt)_2(P(OMe)_3)_2$ are important to note as in both systems with $P(OMe)_3$, the $P(OMe)_3$ ligand substitutes in trans to the Os-Os bond. As this substitution position is consistent between the two complexes, it shows that the presence of bridging ligands in $Os_3(CO)_{10}(\mu\text{-}OEt)_2$ significantly increases its reactivity by the carbonyl ligands trans to the Os-Os bond most labile and likely for substitution to occur at.

2. Reactions of Osmium Carbonyl Complexes of MeCN

The comparison of active sites can also be seen with the addition of acetonitrile, MeCN, to the clusters $Os_3(CO)_{12}$ and $Os_3(CO)_{10}(\mu\text{-}OEt)_2$. Acetonitrile is a labile ligand that is another ligand of focus in this work.

The complex $Os_3(CO)_{12}$ with acetonitrile also forms various products. It is deduced that when $Os_3(CO)_{12}$ is introduced to MeCN and one equivalent of trimethylamine-N-oxide, Me_3NO, at room temperature, under nitrogenous conditions, the monosubstituted product forms, $Os_3(CO)_{11}(MeCN)$[5]. When two equivalents of Me_3NO are added with MeCN, a disubstituted product forms, $Os_3(CO)_{10}(MeCN)_2$ (Figure I.8).

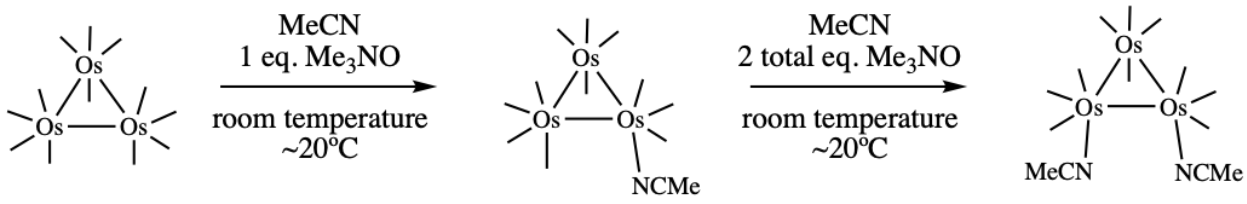

Figure I.8. Reaction scheme of the cluster $Os_3(CO)_{12}$ with MeCN/Me_3NO equivalents.

Tri-substitution of the acetonitrile ligand has not been recorded, which is possible with $P(OMe)_3$. The substitution of the acetonitrile ligand occurs in the axial position, opposite to what is seen with $P(OMe)_3$.

The compound Me_3NO added in one equivalent aids in the substitution process of replacing one carbonyl ligand, for a NMe_3 ligand, and ultimately for an acetonitrile ligand in this reaction[4]. The oxygen in Me_3NO has a negative charge that acts like a nucleophile and attacks the partially positive charged carbon to form CO_2, while the nitrogen of Me_3NO attacks the osmium core to replace the now CO_2 ligand, leaving NMe_3 as the coordinated ligand (Figure I.9). As NMe_3 is a weak ligand, MeCN can readily replace this ligand.

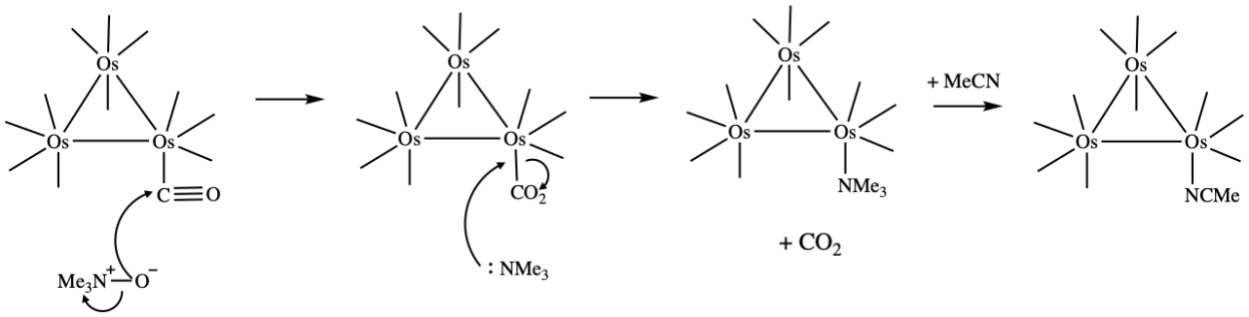

Figure I.9. Mechanism of Me_3NO, substituting a carbonyl ligand with MeCN in the axial position.

Prior research has investigated acetonitrile when reacted with $Os_3(CO)_{10}(\mu\text{-}OEt)_2$. Mary-Ann Pearsall deduced that when bisethoxide is reacted with MeCN and one equivalent of Me_3NO at room temperature, the monosubstituted compound $Os_3(CO)_9(\mu\text{-}OEt)_2(MeCN)$ forms[4]. Me_3NO acts as a guide for the substitution of the CO ligand for a MeCN ligand, as demonstrated in the synthesis of $Os_3(CO)_{12}$ with MeCN/Me_3NO (Figure I.10). The MeCN ligand substitutes in this system in the axial position – and is trans to the bridging ethoxides (not trans to the Os-Os bond as seen with $P(OMe)_3$).

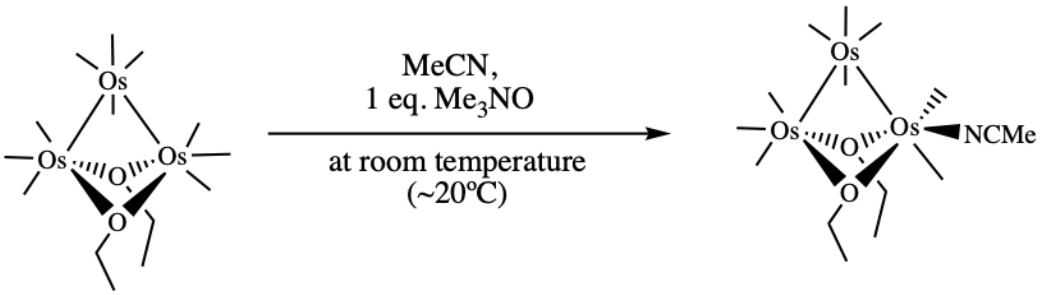

Figure I.10. Reaction scheme of bisethoxide in MeCN with one equivalent of Me_3NO.

When reacting MeCN with $Os_3(CO)_{12}$ and $Os_3(CO)_{10}(\mu\text{-}OEt)_2$, MeCN substitutes in the axial position in both systems. As both systems substitute in the same manner, it shows that the presence of the bridging ethoxides in $Os_3(CO)_{10}(\mu\text{-}OEt)_2$ enhance the complexes overall reactivity with acetonitrile as a coordinating ligand.

Attempts of synthesizing a disubstituted acetonitrile product was attempted by Pearsall through the use of two equivalents of Me_3NO with bisethoxide in MeCN, but results only yielded a monosubstituted product[4]. When this synthesis was repeated by later Pearsall research students (Shannon Higgins), it was proven to consistently yield the monosubstituted acetonitrile product, $Os_3(CO)_9(\mu\text{-}OEt)_2(MeCN)$. This opened questions to whether or not a disubstituted product was possible to synthesize using different reaction conditions.

b. Research Focus

In this research, the direct reaction of $Os_3(CO)_{10}(\mu\text{-}OEt)_2$ in acetonitrile at reflux temperature of 80ºC in hopes of synthesizing the hypothesized product $Os_3(CO)_8(\mu\text{-}OEt)_2(NCMe)_2$ with disubstituted acetonitrile ligands. The starting material of the reflux consisted of bisethoxide and acetonitrile. The purpose of this reaction was to generate a triosmium carbonyl complex with substitution of acetonitrile ligands at the trans positions (Figure I.11).

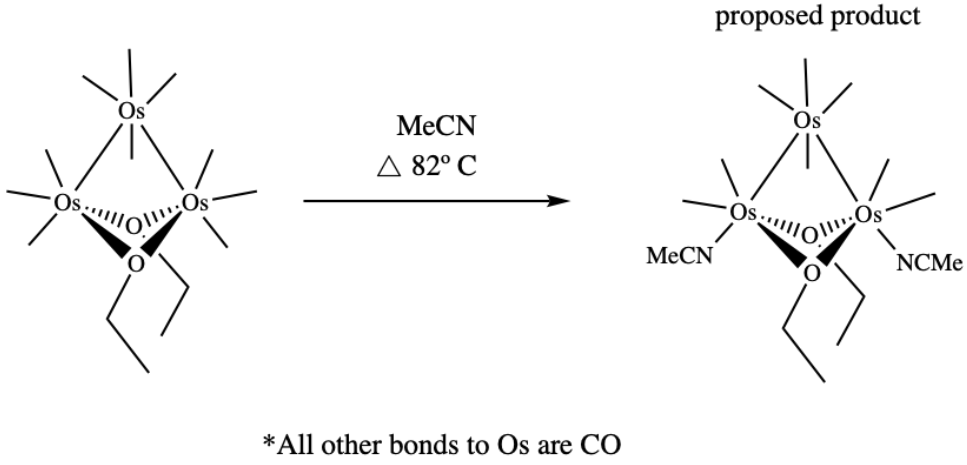

Figure I.11. Reaction scheme of refluxing bisethoxide in acetonitrile, to obtained the hypothesized product $Os_3(CO)_8(\mu\text{-}OEt)_2(NCMe)_2$ through a direct addition of acetonitrile.

As seen in prior research done in the Pearsall lab, it is possible to obtain a disubstituted ligand product with the bridging ligand centers through refluxing bisethoxide in the desired ligand. Thus, this methodology of refluxing bisethoxide in acetonitrile to hopefully obtain a disubstituted acetonitrile product showed reason for further investigation. Not only does this hypothesized complex with disubstituted acetonitrile ligands raise interest synthetically, but also may possess biological interest.

c. Biological Applications of Transition Metal Complexes

Transition metal complexes have been proven to have a range of biological activity. As transition metals are a part of the d-block of the periodic table, they all possess similar chemical reactivity due to their common characteristic of having valence d-electrons. Because these metals react similarly, transition metals have been investigated for potential biological activity. For example, transition metals are featured in some chemotherapy drugs, such as platinum in cisplatin. Located near platinum in the periodic table are elements rhodium and osmium, which are elements of interest in this research. Rhodium complexes have been shown to have biological activity by their ability to bind to DNA, while osmium complexes are being further investigated as literature has proven that osmium carbonyl complexes have biological importance as well[6,1]. Investigating the biological properties of osmium carbonyl clusters further is going to explored in this research. We are curious about synthesized osmium carbonyl complexes synthesized in the Pearsall lab based on published research – as molecules with similar structures react similarly chemically, we propose that the similar complexes may also react similarly biologically.

i. Biological Applications of Osmium Carbonyl Complexes

Leong et al. have investigated the cytotoxicity of different osmium carbonyl cluster complexes against various cancer cell lines[1, 7]. These studies discovered several osmium complexes that displayed anti-cancer properties against these cell lines; $Os_3(CO)_{10}(NCMe)_2$, $Os_3(CO)_{11}(NCMe)$, $Os_3(CO)_{10}(\mu\text{-}H)_2$, $Os_3(CO)_{10}(\mu\text{-}H)(\mu\text{-}OH)$, $Os_6(CO)_{18}$, and $Os_6(CO)_{16}(NCMe)_2$ (Figure I.12). Each of these complexes displayed cytotoxicity to cancerous cells and disrupted the cell cycle. By causing cell death via apoptosis, it is evident that the complexes are biologically reactive. Specifically of these cytotoxic complexes, the complex with the most promising cytotoxic properties was determined to be $Os_3(CO)_{10}(NCMe)_2$. This complex displayed the most significant activity in destroying the cancerous cells most likely due to the coordination of labile bisacetonitrile ($(NCMe)_2$) ligands to the osmium cores that allow reaction of the osmium core to the biological entity (Figure I.13). Another complex with a coordinated labile acetonitrile ligand present is $Os_3(CO)_{11}(NCMe)$, which displayed cytotoxic properties in some cancer lines. The two complexes with bridging centers, $Os_3(CO)_{10}(\mu\text{-}H)_2$ and $Os_3(CO)_{10}(\mu\text{-}H)(\mu\text{-}OH)$ also displayed cytotoxic properties against most cell lines, most likely due to the bridging ligands making the carbonyl ligands on the osmium cores more labile. The hexaosmium carbonyl complexes displayed cytotoxicity levels similar to the bisacetonitrile complex, but contrasts because the hexacarbonyl complexes did induce apoptosis in non-cancerous cells. The cytotoxicity of these osmium complexes were in comparable levels of computed growth inhibition of cells to chemotherapeutic agents tamoxifen and cisplatin, but these osmium clusters were deemed too cytotoxic for normal cells (besides the one complex $Os_3(CO)_{10}(NCMe)_2$ that did not damage non-cancerous cells). The findings revealed that substitutional ligand lability and

the ability to have vacant coordination sites are key factors for osmium carbonyl complexes to be cytotoxic.

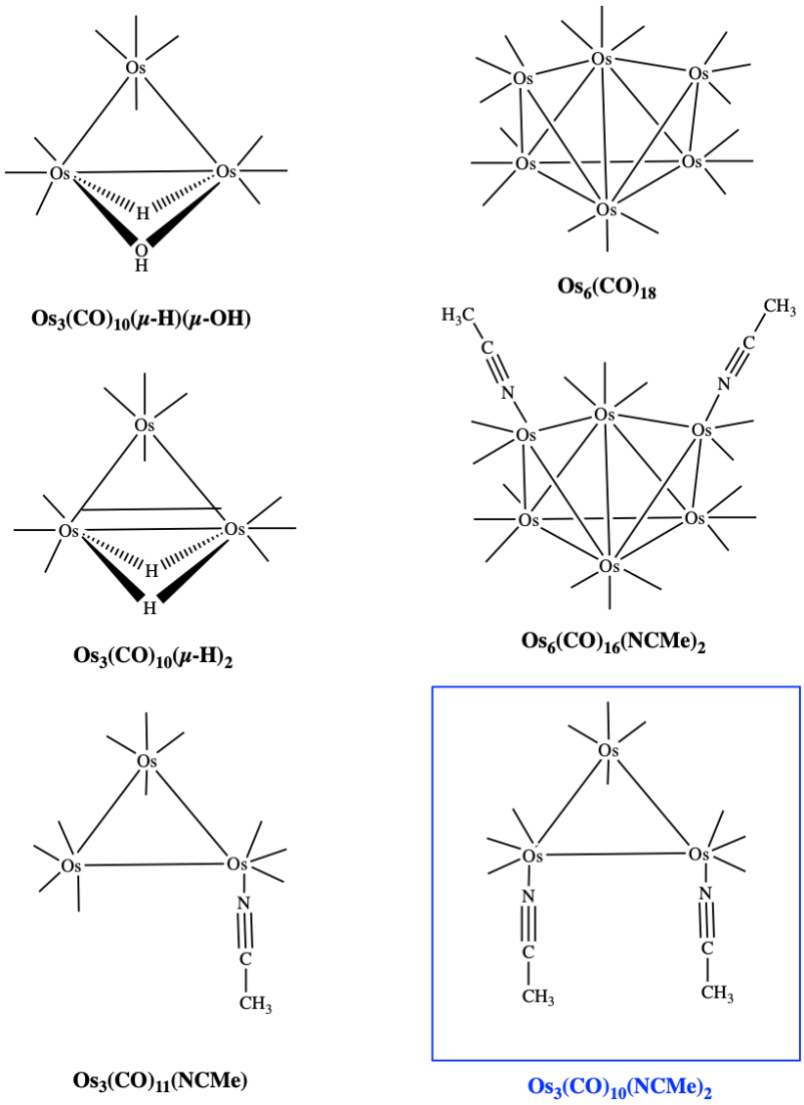

Figure I.12. Structural representations of the complexes deemed to be biologically active against cancer cells[1, 7]. All other bonds to Os are CO ligands. These complexes were tested against several cancer cell lines and were deemed biologically reactive as they induced apoptosis. The most biologically promising molecule, the bisacetonitrile complex (highlighted in blue), was the only complex that was found to be cytotoxic to cancer cells and nonhazardous to non-cancerous cells.

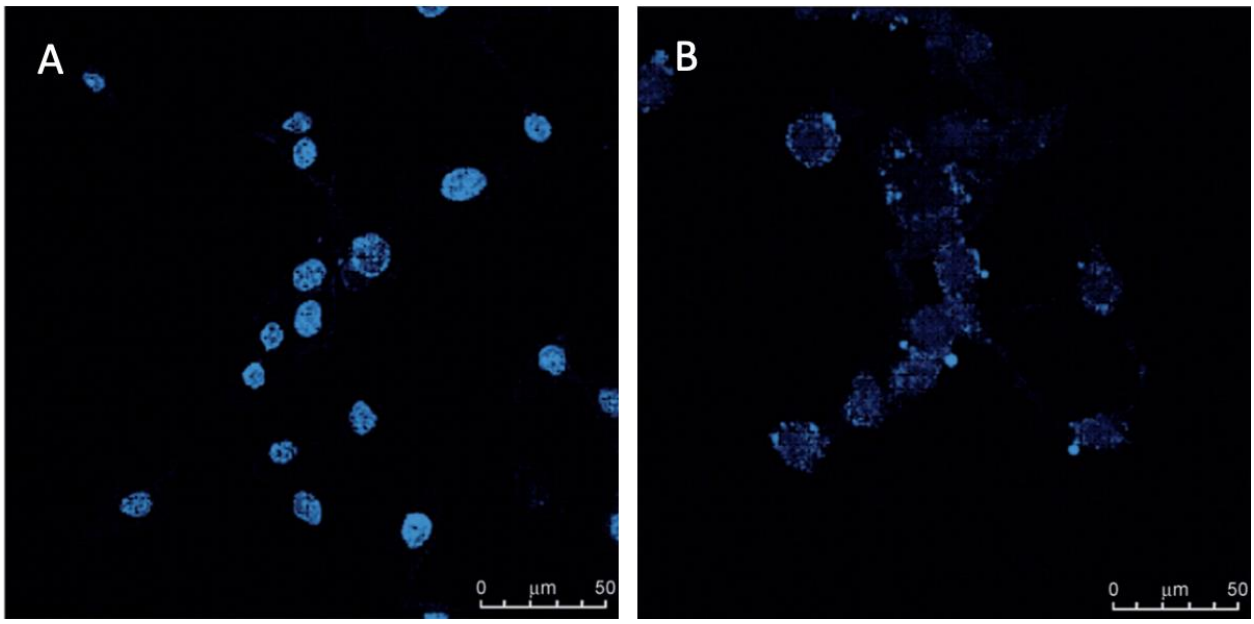

Figure I.13(A,B)[1]. Microscopic look at cancer cells (MCF-7 cells) stained with DAPI (blue) under fluorescent light (image taken from source). This figure visualizes the disruption of mitotic spindle in the cell, as can be seen by comparing **(A)** to **(B)**. (A) Captured image of the control cells, untreated. (B) Image of the same cells after 24 hours when treated with a dosage of $Os_3(CO)_{10}(NCMe)_2$. In (B), the mitotic spindle is disrupted, as the cells look "crushed," indicating that the cell cycle was halted and ultimately resulting in apoptosis.

To further investigate how these complexes tested by Leong induced apoptosis, additional research was conducted to look deeper into the mechanism in how the osmium complexes interact with the cell[8]. The acetonitrile ligand complexes that displayed promising cytotoxic activity, $Os_3(CO)_{10}(NCMe)_2$ and $Os_6(CO)_{16}(NCMe)_2$, were used as the treatment in this study. The complexes were solubilized in DMSO and buffer, then diluted to desired concentrations to test against cancer cells. The cancer cells lines that are being tested undergo a membrane permeabilization preparation step, with the addition of 0.1% Triton X-100 buffer solution, in order to maximize interaction with the cell contents and the osmium complex. When treated with $Os_3(CO)_{10}(NCMe)_2$, the cells show evident disruption of cell cycle as concentration and time increases, and the cell must be permeabilized in order for the osmium complex to

induce apoptosis (Figure I.14). Figure I.14 depicts the disruption of cell cycle via hyperstabilization of microtubules by comparing the experimental treatment – a set concentration of $Os_3(CO)_{10}(NCMe)_2$ solubilized in DMSO – to untreated cancer cells incubated for the same amount of time.

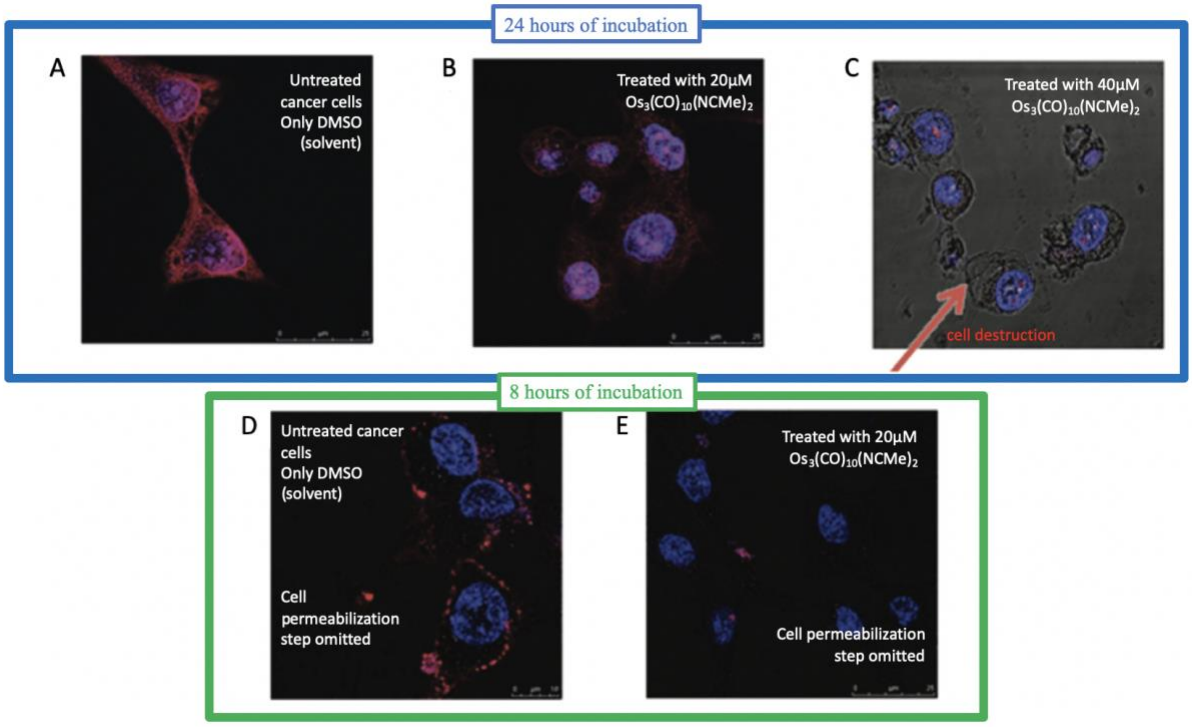

Figure I.14 (A-E)[8]. Fluorescent microscopy of cancer cells (MDA-MB-231) stained with DAPI (blue) and TRM (red). TRM was used to visualize the sulfhydryl residues in the microtubules. The red fluorescence associated with sulfhydryl residues intact to the cell diminishes when increasing concentration of the osmium complex. In (A-C), the images capture the cells after 24 hours of incubation; where (A) is treated with DMSO (control), (B) is treated with 20μM of $Os_3(CO)_{10}(NCMe)_2$, and (C) is treated with 40μM of $Os_3(CO)_{10}(NCMe)_2$. The red arrow in (C) shows the disruption of cells, thus a direct site of microtubule hyperstabilization causing apoptosis. In (D-E), the images capture the cells after 8 hours of incubation, where the cells were stained at 4ºC with no membrane permeabilization step; where (D) is treated with DMSO (control), and (E) is treated with 20μM of $Os_3(CO)_{10}(NCMe)_2$. The fluorescence is diminished from (D) to (E), but no cell disruption occurs.

^{1}H NMR analysis of cells treated with $Os_3(CO)_{10}(NCMe)_2$ showed a multitude of peaks in the metal-hydride region as no distinct osmium carbonyl cluster could be detected, suggesting

that the disubstituted triosmium cluster reacted with intracellular carboxylic acid (R-COOH) and sulfhydryl residues (R-SH) (Figure I.15)[8].

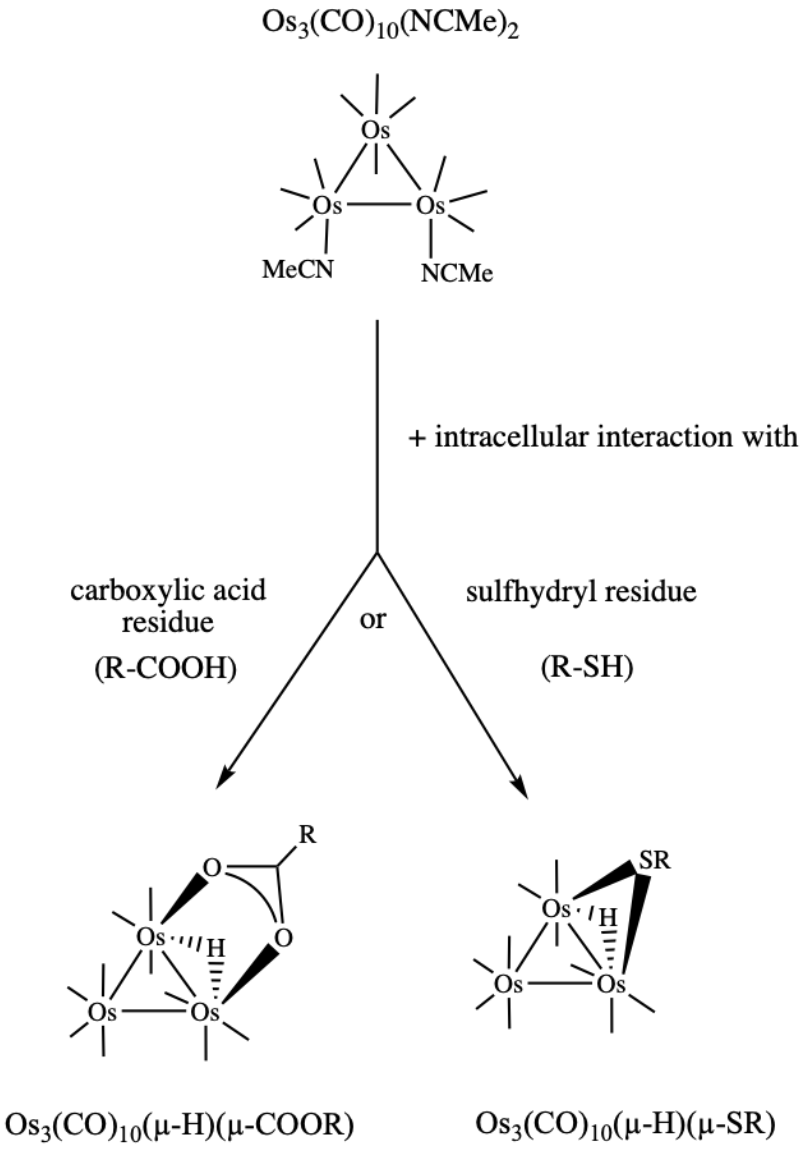

Figure I.15. Flow chart visualization for the reaction of $Os_3(CO)_{10}(NCMe)_2$ with intracellular components to make the complexes proposed to be seen in ^1H NMR, $Os_3(CO)_{10}(\mu\text{-}H)(\mu\text{-}COOR)$ and $Os_3(CO)_{10}(\mu\text{-}H)(\mu\text{-}SR)$[8]. This substitution shows how the lability of the acetonitrile ligands favorably exchange for other functional groups found within a cell. All other bonds to Os are CO ligands.

To further analyze this proposed interaction with intracellular sulfhydryl residues, the cells treated with either osmium cluster were stained in tubulin-FITC antibody to see

microtubule formation of the cells; as microtubules are rich in the sulfhydryl-containing protein tubulin (Figure I.16)[8]. It was observed that the complexes do disrupt tubulin function and ultimately induce apoptosis through the hyperstabilization of microtubules. These results support the notion that the possession of labile ligands and two vacant coordination sites are key for an osmium carbonyl cluster to have significant biological activity.

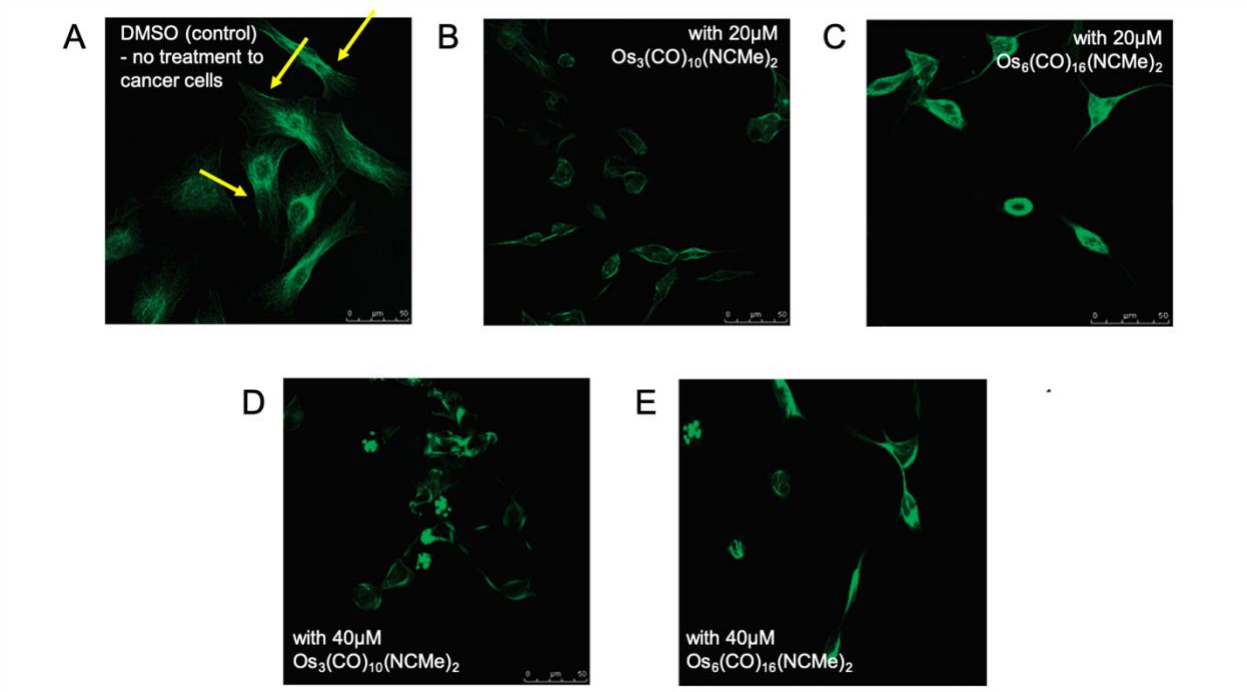

Figure I.16 (A-E)[8]. Microscopic look at cancer cells (MDA-MB-231 cells) stained with tubulin-FITC under fluorescent light (image adapted from source). These images capture the microtubule formation of the cancer cells. In **(A)**, normal cancer cells are shown after 24 hours, where they are treated with DMSO (used as a control, as it is the solvent) with no osmium complex present. The yellow arrows featured in **(A)** highlight the microtubules of the cell, which have a fuzzy, stretched appearance. When looking at **(B-E)** where the cells are treated with osmium complex (image captured after 24 hours of treatment), there are diminishing levels of microtubules present; indicating disruption of tubulin function and ultimately cell growth. In **(B-C)**, the cells were treated with 20μM of $Os_3(CO)_{10}(NCMe)_2$ and $Os_6(CO)_{16}(NCMe)_2$, in DMSO, respectively. In **(D-E)**, the cells were treated with 40μM of $Os_3(CO)_{10}(NCMe)_2$ and $Os_6(CO)_{16}(NCMe)_2$, in DMSO, respectively. With higher concentration, more microtubule disruption was evident in the cells.

In a later study, Leong et. al. looked into complexes with the general formula of $Os_3(CO)_{12-n}(L)_n$, where L is the attached ligand, and investigated how the complex's cytotoxicity relates to its solubility[9]. In prior experiments, poor solubility has been seen to hinder the cytotoxic potential of monosubstituted complexes, like $Os_3(CO)_{11}(NCMe)$, as at some concentrations the complex struggled to solubilize in DMSO and resulted in a weak cytotoxic response[1]. The activity of $Os_3(CO)_{10}(NCMe)_2$ and similar complexes, $Os_3(CO)_{11}(NCMe)$ and $[Os_3(CO)_{11}(NCMe)(\mu\text{-}H)]^+$ are investigated by evaluating their solubilities in DMSO[9]. The protonated compound, $[Os_3(CO)_{11}(NCMe)(\mu\text{-}H)]^+$ had better solubility than $Os_3(CO)_{11}(NCMe)$ in DMSO, indicating that the cationic nature of protonated complex resulted in the acetonitrile being more labile. Due to its lability, it also demonstrated cytotoxic behavior against cancer cells (Figure I.17).

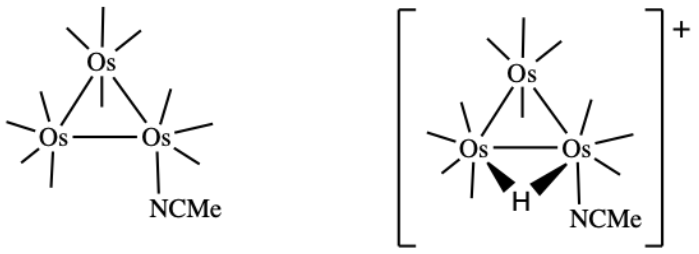

$Os_3(CO)_{11}(NCMe)$ $[Os_3(CO)_{11}(NCMe)(\mu\text{-}H)]^+$

Figure I.17. Structural representations of neutral $Os_3(CO)_{11}(NCMe)$ and protonated $[Os_3(CO)_{11}(NCMe)(\mu\text{-}H)]^+$ complexes[9]. All other bonds to Os are CO ligands.

From this study, it was determined that compounds that possessed good solubility had at least one vacant coordination reaction site available[9]. This potentially indicates that, in order for the osmium complex to have cytotoxic activity, it must have this vacancy or the ability to form one. With good solubility, attached labile ligands will be more likely to be replaced with a

biological moiety (like an interaction with a sulfhydryl residue) because they will be more willing to undergo substitution. Therefore, this study revealed that solubility of a transition metal complex in combination to having labile ligands and vacant coordination sites are important factors to determine if a complex can be biologically reactive.

Leong et. al. continued evaluating the conditions for an osmium complex to be biologically active reacting $Os_3(CO)_{10}(NCMe)_2$ with carboxylated chalcone and benzaldehyde derivates and analyzing the product's cytotoxicity against cancer cells[10].

Chalcones are a known biological entity as they possess anti-cancer, anti-inflammatory, anti-microbial, and other important functions in medicinal chemistry[11]. A parent chalcone consists of two aromatic rings joined together by a three-carbon α,β-unsaturated carbonyl system (Figure I.18). By reacting the already biologically active complex $Os_3(CO)_{10}(NCMe)_2$ with a compound with biological properties raises question on how it will affect the complex's reactivity with cells[10].

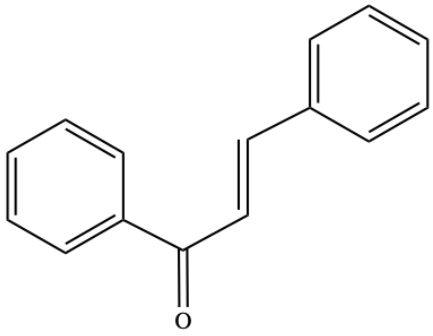

Figure I.18. Parent structure of a chalcone.

Derivatives of the parent structure of the chalcone are created in this study where alcohol groups are added to the aromatic ring (seen in Figure I.20). The carboxylated chalcone or benzaldehyde reacts with the osmium cluster by replacing the two acetonitrile ligands to form a

bridged ligand from the carboxylate moiety of the organic compound (Figure I.20), with the general formula of $Os_3(CO)_{10}(\mu\text{-}H)(\mu\text{-}COOR)$ (Figure I.19)[10].

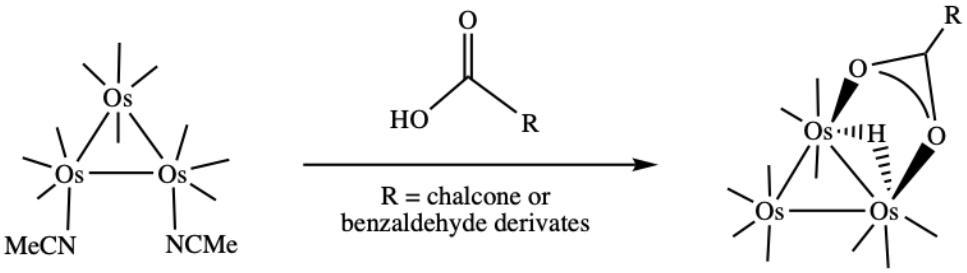

Figure I.19. Reaction scheme of $Os_3(CO)_{10}(NCMe)_2$ with a carboxylated chalcone or benzaldehyde to form $Os_3(CO)_{10}(\mu\text{-}H)(\mu\text{-}COOR)$[10]. All other bonds to Os are CO ligands.

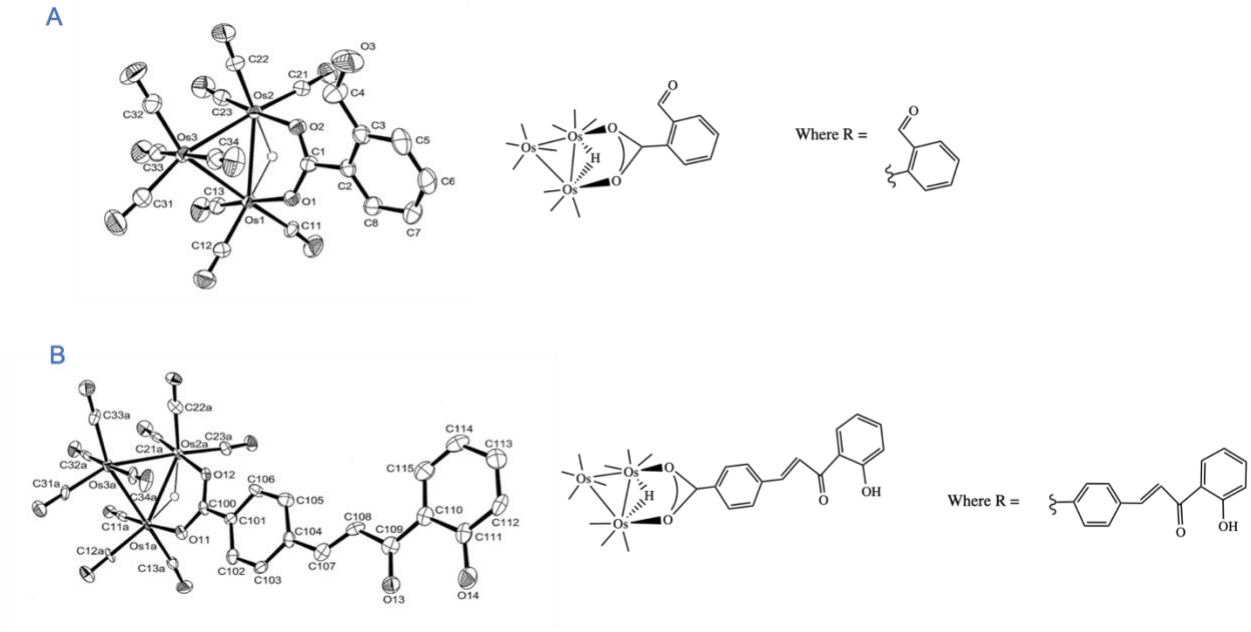

Figure I.20(A,B)[10]. X-ray crystallography structures of $Os_3(CO)_{10}(\mu\text{-}H)(\mu\text{-}COOR)$ with R as a benzaldehyde (a) and a chalcone (b) derivates. Crystal structures obtained directly from source. All other bonds to Os are CO ligands.

It was found that the carboxylated chalcone and benzaldehyde derivative products were not cytotoxic to the cancer cell line while the $Os_3(CO)_{10}(NCMe)_2$ complex remained cytotoxic[10]. It was hypothesized that substitution of the labile acetonitrile ligands with the chalcone ligand affected the interaction of the osmium complex with the intracellular residues (sulfhydryl and carboxylate). These results suggests that two labile ligands must be located at the complex's

osmium core (attached to the Os) - either bridging or directly attached - to have biological reactivity and that substitution of these two ligands prior to interaction with a cell could impact the complex's biological properties.

Leong et al. continued their work on the biological applications of osmium carbonyl clusters by investigated the nature of how the cytotoxic complexes interact with cancer cells even deeper[12]. This study determined that the osmium carbonyl complex $Os_3(CO)_{10}(MeCN)_2$ interacts with cancer cells via a cysteine amino acid residue.

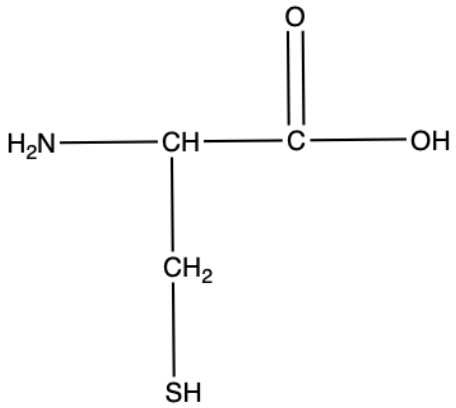

Figure I.21. Structure of the amino acid cysteine[13].

The thiol (-SH) present in the amino acid cysteine creates a target for interaction, as tubulin of cells are rich in sulfhydryl residues (Figure I.21). From previous research done by Leong et. al, it was shown that that $Os_3(CO)_{10}(MeCN)_2$ disrupts tubulin function of cells[8]– thus leading to the conclusion in this study that the reactive disubstituted complex more specifically interacts with cysteine residues of the cells[12]. Additional amino acids that engaged with the cytotoxic cluster were aspartic acid and glutamic acid, with cysteine being the most reactive. This research gives osmium carbonyl complexes even more reason to be investigated further as biological agents.

ii. Biological Applications of Rhodium Complexes

As previously noted, another transition metal that has shown biological properties is rhodium. In particular, dirhodium complexes have shown biological properties in their ability to bind to DNA[6, 14].

Research done by Dunham in 2005 investigated the biological activity of dirhodium carboxylate complexes[6]. The complexes $Rh_2(O_2CCH_3)_4(H_2O)_2$, $[Rh_2(O_2CCH_3)_2(MeCN)_6]^{2+}$, and $Rh_2(O_2CCF_3)_4$ were evaluated in their interaction with double stranded DNA (Figure I.22).

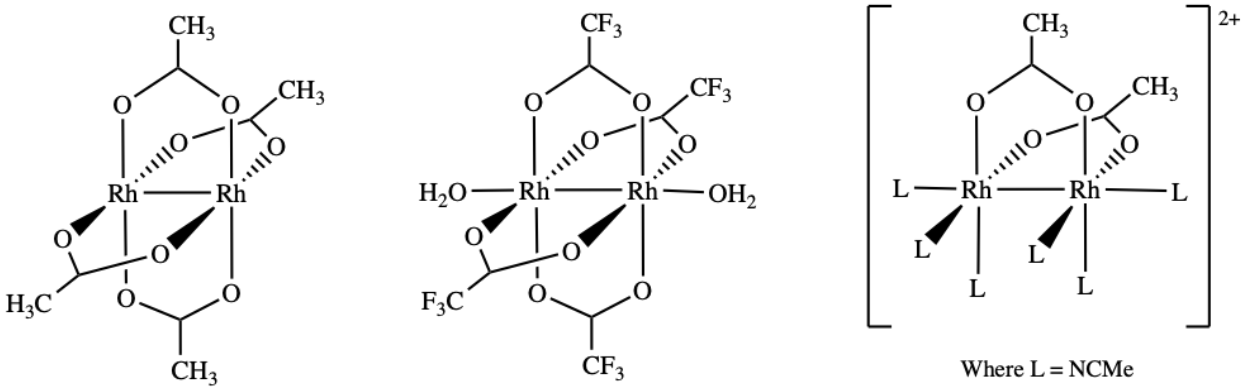

Figure I.22. Structures of dirhodium carboxylate complexes tested against double-stranded DNA.

The kinetics of each complex's binding to the double-stranded DNA was measured through UV-vis spectroscopy and Graphite Furnace Atomic Absorption spectroscopy, where the percentage of rhodium complex bound was measured over the reaction time. Through this analysis, it was determined that the complex $Rh_2(O_2CCF_3)_4$ had the fastest binding interaction; then $[Rh_2(O_2CCH_3)_2(MeCN)_6]^{2+}$; and $Rh_2(O_2CCH_3)_4(H_2O)_2$ showed extremely little binding activity in comparison to the other complexes. When the complexes interacted with the double-stranded DNA, each complex was found to form rhodium-DNA adducts, and created interstrand crosslinks. Interstrand crosslinks are toxic DNA lesions that prevent transcription, replication,

and DNA strand separation; where chemotherapy drugs are often agents that induce interstrand crosslinks[15]. This study showed that through the interaction of the complexes proven to bind to double-stranded DNA and creating crosslinks that there is biological potential of the dirhodium carboxylate complexes to be evaluated as anti-cancer agents[6]. It also revealed that various ligands attached to the rhodium cores alter the dirhodium complex's kinetic properties when binding to double-stranded DNA, as each complex varied in lability due to differences in leaving group behavior and ultimately resulted in different binding rates to double-stranded DNA.

In 2011, Dunham expanded on the DNA binding properties of dirhodium complexes by looking at carboxyamidate complexes[14]. Three dirhodium carboxyamidate complexes are produced during the synthesis of $Rh_2(HNOCCF_3)_4$, from $Rh_2(OOCCH_3)_4$ and trifluoroacetamide; which these complexes are $Rh_2(\mu\text{-}L)(\mu\text{-}HNOCCF_3)_3$ where L is $(HNOCCF_3)^-$, $(OOCCF_3)^-$, or $(OOCCH_3)^-$ (Figure I.23).

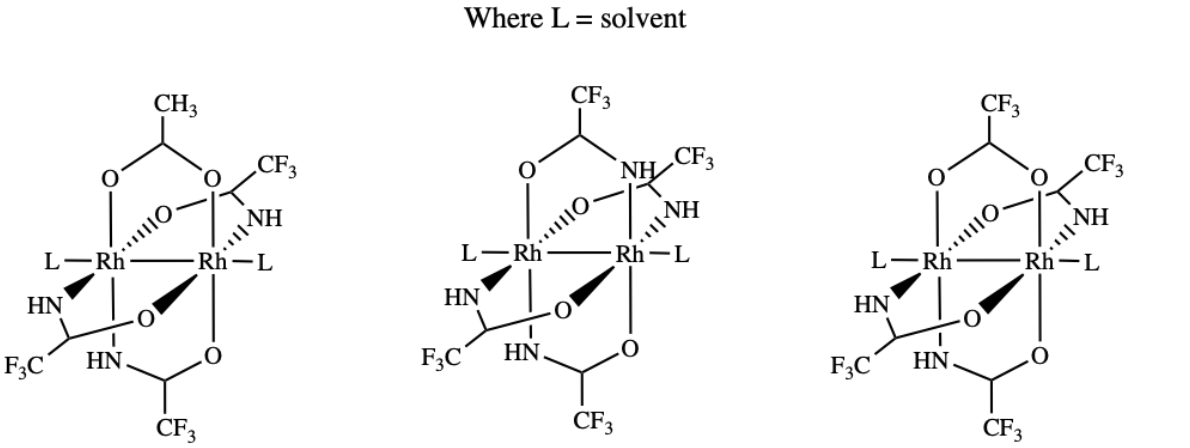

$Rh_2(\mu\text{-}OOCCH_3)(\mu\text{-}HNOCCF_3)_3$ $Rh_2(\mu\text{-}HNOCCF_3)(\mu\text{-}HNOCCF_3)_3$ $Rh_2(\mu\text{-}OOCCF_3)(\mu\text{-}HNOCCF_3)_3$

Figure I.23[14]. Structure of the three dirhodium carboxyamidate complexes analyzed.

The characterization of these compounds revealed that a single ligand change out of one of the four bridging ligand positions greatly alters the DNA-binding kinetics of the compound[14]. The binding rates of each complex were different due to the differences in one bridging ligand,

where it was found that the (μ-$OOCCF_3$) and the (μ-$OOCCH_3$) complexes had similar binding rates. It was determined that complexes with acidic bridging ligands have faster DNA-binding kinetics due to the ligands being better leaving groups and possessing more lability; and more specifically, a single bridging trifluoroacetate ligand (μ-$OOCCF_3$) present indicated faster binding[14]. Therefore, these results indicate that changes in the bridging ligand environment can lead to dirhodium complexes having better catalytic and biological properties.

These complexes are relevant to our work because osmium and rhodium display similar chemical reactivity, which proposes question the metals possess similar biological activity. As osmium carbonyl complexes have been shown to demonstrate biological activity as cancer agents, it generates interest in seeing if osmium carbonyl complexes may behave similarly to dirhodium complexes. Parallels in structure between both transition metal complexes create curiosity in investigating the biological properties of complexes synthesized by the Pearsall lab.

iii. Proposed Biological Activity of $Os_3(CO)_{10-x}(\mu\text{-}OEt)_2(MeCN)_x$

Though we are unsure of the biological activity of bisethoxide and derivate products, all the findings deduced from the multiple published studies on osmium carbonyl clusters by Leong throughout the years allow us to believe that the proposed products from bisethoxide and various reagent syntheses have the potential to be biologically active[1]. Building off of these proven cytotoxic complexes, the complexes with acetonitrile coordinated ligands were further studied and proven to be more biologically interesting than others. As coordinated acetonitrile ligands to osmium carbonyl clusters and bridged-ligand carbonyl complexes are both biologically active, parallels can be drawn to provide belief that a bridged-ethoxide osmium carbonyl complex ($Os_3(CO)_{10-x}(\mu\text{-}OEt)_2(MeCN)_x$) will be biologically active.

Future work includes the analysis of the biological activity of synthesized osmium carbonyl complexes – specifically $Os_3(CO)_{10-x}(\mu\text{-}OEt)_2(MeCN)_x$. One factor to consider is the solubility of the complex $Os_3(CO)_{10-x}(\mu\text{-}OEt)_2(MeCN)_x$, as a cluster must be soluble in order to be biologically active[9]. The complex will be sent to Dr. Shari Dunham at Moravian College, to test the complex's ability to bind to DNA will be evaluated. Further investigation is needed to see how these bridging ethoxide groups and coordinated acetonitrile ligands play a role in the potential biological activity of this compound.

3. Methods

a. FT-Infrared Spectroscopy

One way to identify transition metal complexes is through Infrared Spectroscopy (IR). In the study of transition metal carbonyls - in specific, osmium carbonyl clusters - the focus is on the frequency where a carbonyl ligand coordinated to a metal can be found, which typically is the 1600 cm^{-1} to 2200 cm^{-1} wavelength range. To analyze a product in the lab, the IR spectra obtained of that product is compared to the IR of our parent molecule, $Os_3(CO)_{12}$, to see if a reaction has occurred. This is done frequently throughout a synthesis process to identify if a change in product is occurring and to see if the reaction is proceeding. If a new peak pattern arises on the IR (in comparison to the parent molecule spectrum), one can deduce that the carbonyl (CO) ligand symmetry of the molecule has changed because a reaction has taken place. Changes found in the peak frequencies indicate different stretching patterns of the CO ligands, indicating loss of carbonyl ligands, or how they experience different vibrational modes based on additional ligands that are coordinated to the same osmium as the absorbed carbonyls. The more symmetrical molecules are, the fewer absorption peaks will occur. Because $Os_3(CO)_{12}$ has a high

degree of molecular symmetry, there are less peaks compared to a complex that is less symmetrical, like $Os_3(CO)_{10}(OEt)_2$ (Figure M.1). Infrared spectrums are taken using a NaCl solution cell, where the reaction mixture of interest is loaded into the cell and placed into the infrared spectrometer to obtain a spectrum.

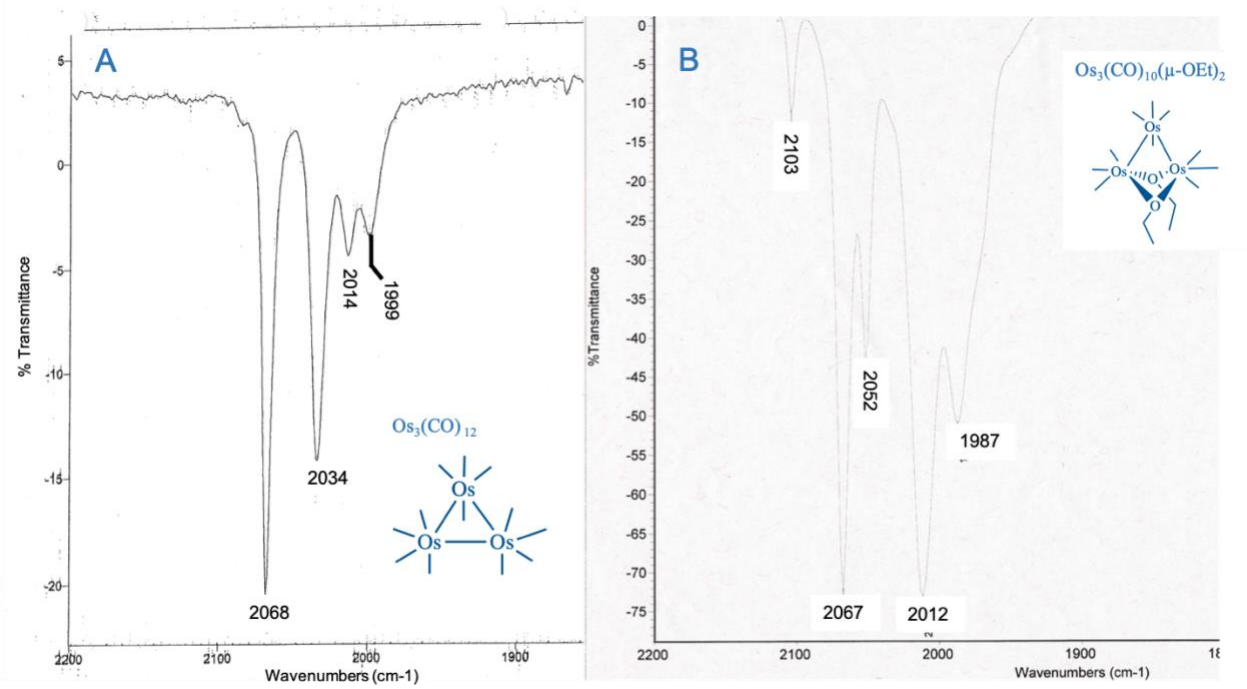

Figure M.1(A,B)[16]. Infrared spectra comparison of the spectrum of $Os_3(CO)_{12}$ (A) to the spectrum of $Os_3(CO)_{10}(\mu\text{-}OEt)_2$ (B). Peak shifts and patterns are observable when comparing the two complexes that have a difference in attached carbonyl ligands, molecular symmetry, and reactivity. Spectra are measured in percent transmittance.

b. Thin Layer Chromatography

Reaction progression and products are also analyzed through Thin Layer Chromatography (TLC), which creates a visual separation of compounds in a mixture based on their polarity and intermolecular forces. For a TLC conducted on an experimental reaction, the reactant mixture is spotted onto a thin plate that has a layer of silica, which acts as the polar

stationary phase; then the plate is inserted into a solvent system that serves as a mobile phase. The mobile phase consists of two solvents: less polar hexanes, and more polar ethyl acetate (or dichloromethane). The solvent will move up the plate and carry compounds to different distances based on their affinity for the solvent used, separating compounds that differ in polarity. So, a more non-polar compound will travel farther in a more non-polar solvent from its initial position than a more polar compound would. Once the compounds are plated and time has been allowed for the solvent system to move through the gel, the plate is removed from the TLC chamber and analyzed under UV lamp, as fluorescent spots of the analytes can be observed.

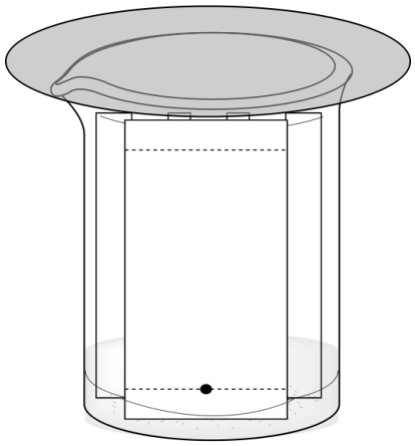

Figure M.2. TLC set up. Representation of TLC chamber using a glass beaker with mobile phase solvent system, filter paper, and the TLC chip once spotted. The chamber is covered with a watch glass.

To quantitatively compare compounds in a mixture, we can use the R_f (retention factor) value, which can be calculated by measuring the distance the compound traveled and dividing it by the total distance the mobile phase traveled up the plate. Compounds can be identified by the R_f values obtained. The formula for calculating this value is seen in Figure M.3. In the synthesis of bisethoxide and derivative reactions, TLC is used continuously to classify, separate, and ensure that products are being formed.

$$Rf = \frac{\text{distance traveled by analyte}}{\text{distance traveled by solvent}}$$

Figure M.3. Formula for determining retention value of an analyte on a TLC plate.

c. Nuclear Magnetic Spectroscopy

Another way to analyze osmium carbonyl compounds is through Nuclear Magnetic Spectroscopy (NMR). Specific information can be derived from a ^{1}H-NMR that helps identify and properly characterize the complex in testing; specifically, the number of unique chemically unique hydrogens in the molecule, the chemical shift of the protons, the integration, and the multiplicity of hydrogens. The number of signals that arise correspond to the number of protons with varying chemical environments within the molecule. The chemical shift of these protons can help characterize their proximity to electronegative groups in a molecule, by seeing whether the protons are more downfield (closer to electronegative groups) or more upfield (farther from electronegative groups). The integration of each peak corresponds to the amount of hydrogens in that specific chemical group. The multiplicity of a peak shows the splitting of a signal, as it gives information of the number of non-chemically equivalent hydrogen neighbors (n+1 rule). Characterizing specific information that can be derived from a NMR spectrum confirms product formation, multiple products in a mixture, and reaction progression or success.

d. Synthesis Techniques

One common method used to conduct reactions in the lab is through refluxing. To react a specific reagent with bisethoxide, it is typically done through a reflux. Other reflux reactions occur in the lab when reacting bisethoxide derivative products with other reagents as well.

Reflux reactions are conducted under nitrogenous conditions. The reflux setup consists of a round bottom flask (containing bisethoxide, the reagent being added, and a stir bar). This round bottom flask is attached to a water condenser, which is capped with a nitrogen gas feeding tube. The water condenser is used to keep the reaction from boiling off and to conserve product while the reaction mixture is boiling, and the stir bar keeps the reaction mixture from bumping. This setup is placed on a stir plate with a heating mantle, to mix and heat the reaction mixture to a steady reflux. The refluxing reaction is monitored through frequent IRs and TLCs to track reaction progress and product formation.

Another method utilized in the lab is a microwave synthesis. A reaction involving the microwave allows for reactions with larger, sterically bulky reagents to proceed with better yield and faster reaction times[17]. This method of using a microwave is used to create $Os_3(CO)_{10}(\mu\text{-}OEt)_2$ from $Os_3(CO)_{12}$, by microwaving triosmium decacarbonyl with solid iodine and cyclohexane. It is an effective reaction aid because the microwave supplies electromagnetic energy and heat that ultimately increases the molecular rotation of the compounds in the reaction mixture and likeliness for molecules to collide in proper orientation to produce products.

4. Experimental

a. Experimental synthesis of triosmium decacarbonylbisethoxide, $Os_3(CO)_{10}(\mu\text{-}OEt)_2$

To a 35 mL microwave tube, 201 mg of triosmium dodecacarbonyl ($Os_3(CO)_{12}$, 0.2217 mmol), 0.062 g of I_2 (0.2443 mmol), and 14 mL of cyclohexane were added and dissolved in a 35 mL microwave tube. With a stir bar added, the solution-containing tube was microwaved at 150ºC, at 300 watts and 275 psi for ten minutes (using the load Os3I2 programmed method). The reaction mixture was transferred to a 250 mL round-bottom flask, and cyclohexane was removed by rotary evaporation to get a solid product. Dichloromethane (CH_2Cl_2) was added to dissolve the product. IR of the product was obtained; results showed the product was $Os_3(CO)_{10}(I)_2$ with peaks of 2110 cm^{-1}, 2074 cm^{-1}, 2064 cm^{-1}, 2021 cm^{-1}, 2007 cm^{-}`, and 1985 cm^{-1} present.

100 mL of ethanol was added to the round-bottom flask containing $Os_3(CO)_{10}(I)_2$ obtained above, and 0.204 g alumina (Al_2O_3) (2.001 mmol) was added to the solution. The solution was heated at 78ºC and monitored with IR spectroscopy and thin layer chromatography (20% ethyl acetate: 80% hexanes) for 3.5 hours. The reaction was complete when the IR showed the same pattern obtained for $Os_3(CO)_{10}(I)_2$, but with new shifted peaks signature to bisethoxide. The 2110 cm^{-1} peak found in the diiodide was replaced by peaks of 2067 cm^{-1} and 2103 cm^{-1} (signature to bisethoxide). When the reaction was determined to be complete, the product was filtered to eliminate excess alumina before removing ethanol to obtain a solid product. IR was obtained in CH_2Cl_2, showing that the product was impure and had a 2034 cm^{-1} peak consistent with $Os_3(CO)_{12}$. A column (20% ethyl acetate/hexanes) was performed to further purify the compound. Fractions were then analyzed via TLC and combined. The solvent was removed by rotary evaporation and 20 mL dichloromethane was added to reform the product for IR. Peaks present are 2103 cm^{-1}, 2067 cm^{-1}, 2052 cm^{-1}, 2012 cm^{-1}, and 1987 cm^{-1}. Yield analysis

determined that the product obtained by the reaction was triosmium decacarbonylbisethoxide, $Os_3(CO)_{10}(\mu\text{-}OEt)_2$, (165mg, 0.0001754 mol, 82.1% yield).

Procedure was repeated multiple times in success during this research and found the same results (peaks consistent with bisethoxide) with varying successful percent yields.

b. Experimental synthesis attempt of $Os_3(CO)_8(\mu\text{-}OEt)_2(NCMe)_2$

To a 100 mL round-bottom flask, 10 mg $Os_3(CO)_{10}(\mu\text{-}OEt)_2$ was dissolved (~20 mL NCMe) in HPLC grade acetonitrile. Reaction mixture was stirred and heated at ~80ºC under nitrogenous conditions for approximately 2 hours. The reaction was monitored through IR analysis. At the high temperature and time of reflux, IR analysis resulted in peaks 2092 cm^{-1}, 2078 cm^{-1}, 2072 cm^{-1}, 2053 cm^{-1}, 2000 cm^{-1}, 1987 cm^{-1}, and 1907 cm^{-1}. The high temperature reaction mixture was cooled to room temperature in MeCN solvent (IR peaks: 2103 cm^{-1}, 2092 cm^{-1}, 2069 cm^{-1}, 2000 cm^{-1}, 1990 cm^{-1}, 1958(sh) cm^{-1}, and 1917 cm^{-1}). Solvent was evaporated and product was dissolved in dichloromethane (CH_2Cl_2) (IR peaks: : 2104 cm^{-1}, 2092 cm^{-1}, 2069 cm^{-1}, 2004 cm^{-1}, 1994 cm^{-1}, 1978(sh) cm^{-1}, 1958(sh) cm^{-1}, and 1919 cm^{-1}) TLC analysis was inconclusive in various solvent systems. CH_2Cl_2 was evaporated off and solid was vacuum pumped under nitrogen for several hours. A small sample of product was removed and deuterated chloroform ($CDCl_3$) was added to the product in an NMR tube. ^1H NMR spectra were taken directly after synthesis and approximately 36 hours later. Product confirmed by ^1H NMR (peaks at ~4ppm (m), coordinated acetonitrile; approx. 2:1 ethoxide to acetonitrile ligand ratio) and IR analysis that $Os_3(CO)_9(\mu\text{-}OEt)_2(MeCN)$ is obtained. Procedure was repeated multiple times and held consistent with obtained IR data.

c. Experimental synthesis of $Os_3(CO)_9(\mu\text{-}OEt)(MeCN)$ with $P(OMe)_3$

Directly after the synthesis of $Os_3(CO)_9(\mu\text{-}OEt)(MeCN)$ through the reflux of $Os_3(CO)_{10}(\mu\text{-}OEt)_2$ in HPLC grade acetonitrile (seen in *b*), one drop of trimethylphosphite, $P(OMe)_3$, was added to $Os_3(CO)_9(\mu\text{-}OEt)(MeCN)$ in CH_2Cl_2. Reaction was stirred at room temperature under N_2 gas, and monitored by IR. At initial addition of $P(OMe)_3$ (t=0), new IR peaks were overserved (IR peaks: 2103 cm^{-1}, 2086 cm^{-1}, 2068 cm^{-1}, 2047 cm^{-1}, 2010 cm^{-1}, 1996 cm^{-1}, 1977 cm^{-1}, 1961 cm^{-1}, and 1941 cm^{-1}). IR confirms product formation of $Os_3(CO)_9(\mu\text{-}OEt)_2(P(OMe)_3)$ at t = 0 hrs. The reaction was monitored for approximately 36 hours stirring at room temperature under N_2 gas. At t = 36 hrs, IR analysis showed a new peak pattern (IR peaks: 2104 cm^{-1}, 2090 cm^{-1}, 2067 cm^{-1}, 2062 cm^{-1}, 2052 cm^{-1}, 2009 cm^{-1}, 1976 cm^{-1}, and 1941 cm^{-1}). Present peaks display that the product is now $Os_3(CO)_8(\mu\text{-}OEt)_2(P(OMe)_3)_2$. TLC analysis in 50 CH_2Cl_2: 50 hexanes showed two spots in the sample, one corresponding to bisethoxide (Rf=0.57) and one of $Os_3(CO)_8(\mu\text{-}OEt)_2(P(OMe)_3)_2$ (Rf=0.34). Procedure was repeated multiple times and held consistent with obtained IR data and results.

d. Experimental synthesis of $Os_3(CO)_9(\mu\text{-}OEt)(MeCN)$ with PPh_3

Directly after the synthesis of $Os_3(CO)_9(\mu\text{-}OEt)(MeCN)$ through the reflux of $Os_3(CO)_{10}(\mu\text{-}OEt)_2$ in HPLC grade acetonitrile (seen in *b*), one drop of trimethylphosphite, $P(OMe)_3$, was added to $Os_3(CO)_9(\mu\text{-}OEt)(MeCN)$ in CH_2Cl_2. Reaction was stirred at room temperature under nitrogenous conditions. The reaction was monitored by IR, where IR analysis of this reaction was inconclusive as no complete peak pattern could be assigned to identifiable osmium complexes.

5. Results and Discussion

i. Reaction of $Os_3(CO)_{10}(\mu\text{-}OEt)_2$ in acetonitrile

In this research, the direct reaction of $Os_3(CO)_{10}(\mu\text{-}OEt)_2$ in acetonitrile at reflux was investigated in hopes of synthesizing the proposed product $Os_3(CO)_8(\mu\text{-}OEt)_2(NCMe)_2$ with disubstituted acetonitrile ligands. The goal of this reaction was to generate a triosmium carbonyl complex with substitution of acetonitrile ligands at the trans positions (Figure R.1).

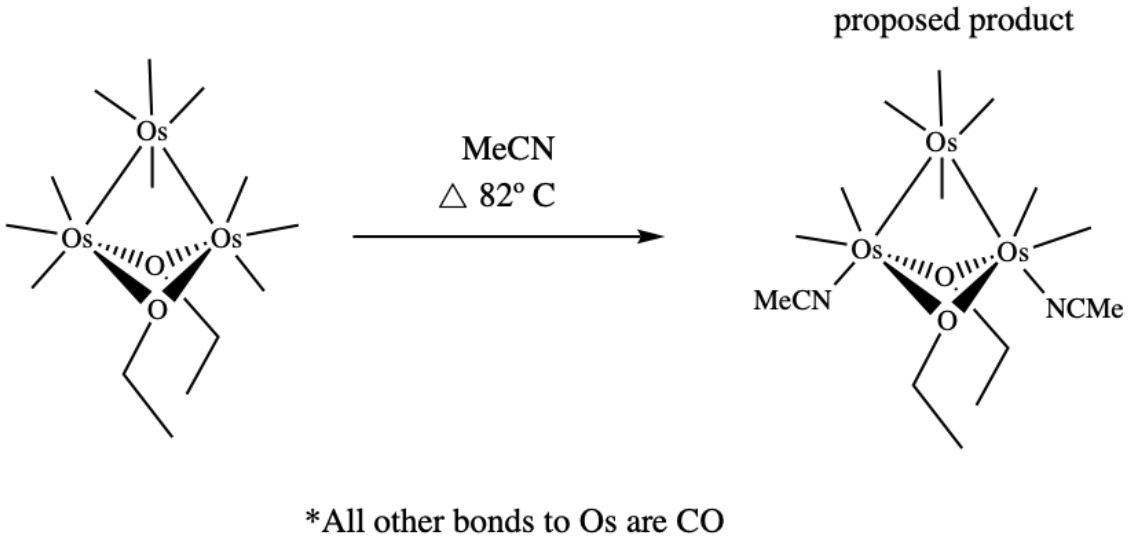

Figure R.1. Reaction scheme of refluxing bisethoxide in acetonitrile, to obtained the hypothesized product $Os_3(CO)_8(\mu\text{-}OEt)_2(NCMe)_2$ through a direct addition of acetonitrile.

The reaction progression of bisethoxide is monitored through infrared spectroscopy. The initial reaction of bisethoxide with acetonitrile, prior to refluxing, is shown in Figure R.2.

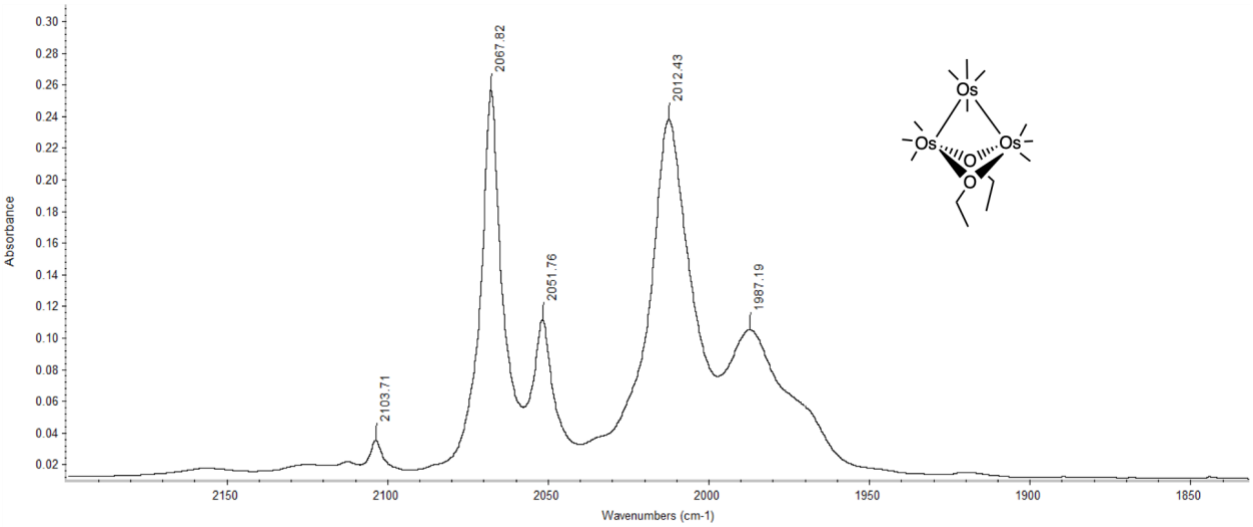

Figure R.2. Infrared spectrum of the acetonitrile and bisethoxide reaction at starting time, prior to start of reflux. Measured in absorbance.

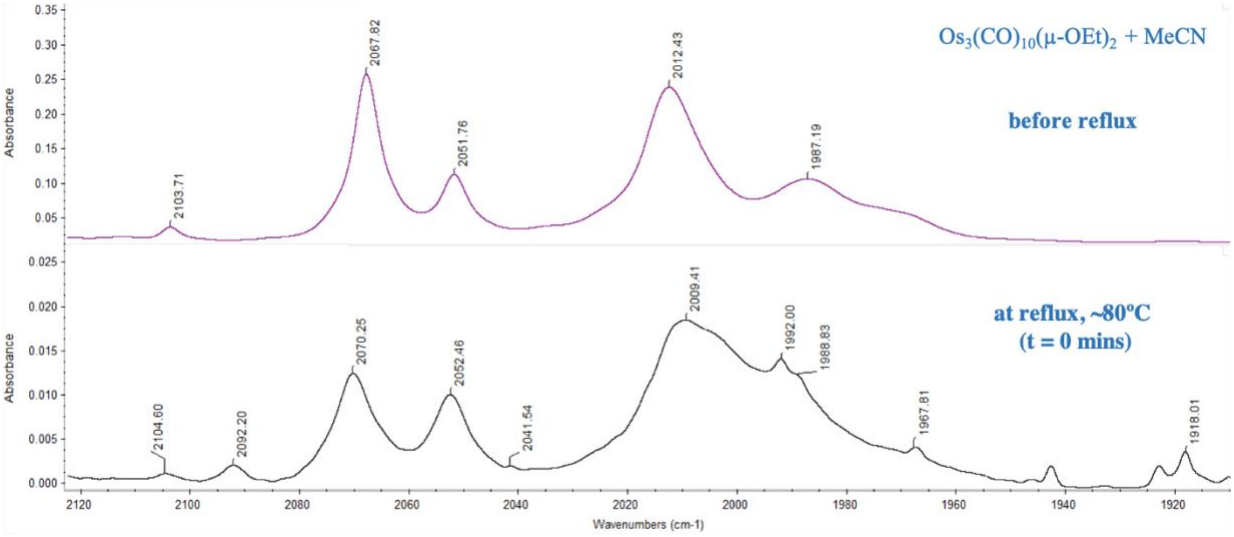

Figure R.3. Stacked spectrum comparing the reaction mixture prior to reflux ($Os_3(CO)_{10}(\mu\text{-}OEt)_2$ and acetonitrile, no heat) (top) to $Os_3(CO)_{10}(\mu\text{-}OEt)_2$ reflux in acetonitrile, at boiling point (bottom). Measured in absorbance.

Changes in an IR, either peaks shifting wavenumbers or the disappearance or appearance of peaks, indicate that a reaction is occurring. Figure R.3 shows an infrared spectrum of the reaction at the start of reflux (bottom), compared to the reaction prior to reflux (top). Wavelength

differences are indicated by the peak shifting away from the blue lines at wavelengths 2012 cm-1 and 1987 cm^{-1} of bisethoxide, which were observable at boiling point. It is apparent that the bisethoxide peak of 2012 cm^{-1} disappeared while the 2009cm^{-1}, 1992cm^{-1} and 1987cm^{-1} peaks grow in. The 2103 cm^{-1} and 2067 cm^{-1} peaks of bisethoxide also disappear, while new peaks of 2092 cm^{-1} and 1967 cm^{-1} grow in.

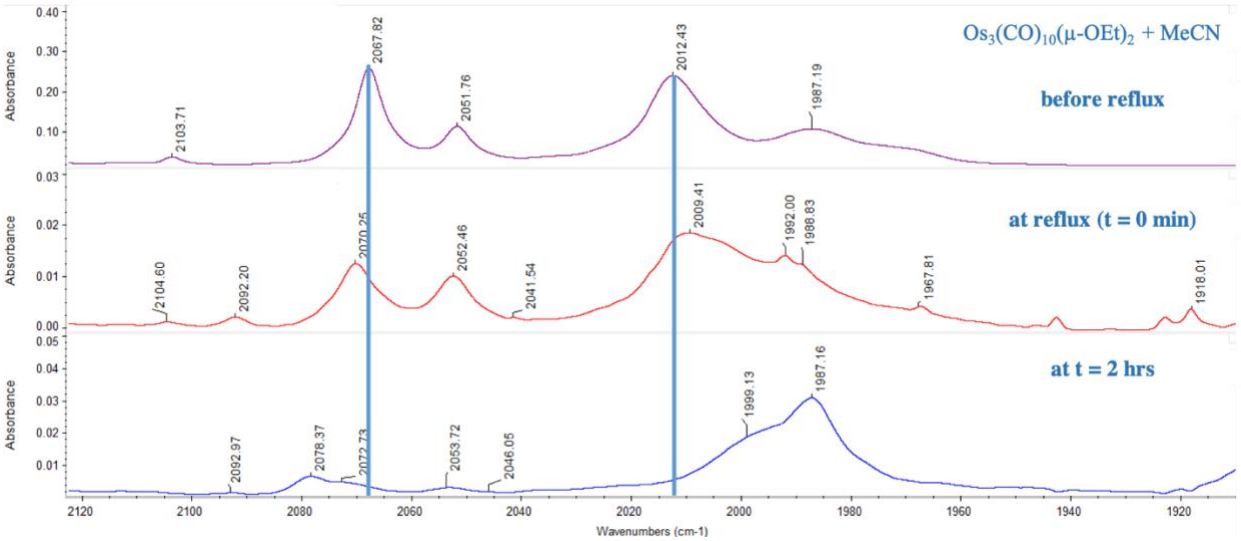

Figure R.4. Stacked spectrum comparing the initial reaction mixture (top), to boiling point (t = 0 mins, middle), to maximum time refluxed (t = 2 hours, bottom). Measured in absorbance.

The reflux was stopped once there was believed to be total consumption of $Os_3(CO)_{10}(\mu\text{-}OEt)_2$, based off of the disappearance of the 2103 cm^{-1} and 2067 cm^{-1} peaks in the IR. Wavelength differences are indicated by a peak shifting away from the blue lines placed at bisethoxide's 2067 cm^{-1} and 2012 cm^{-1} peaks (Figure R.4). Shown in Figure R.4, the notable peaks observed after 2 hours of reflux (maximum time) were 2092 cm^{-1}, 2078 cm^{-1}, 2053 cm^{-1}, 2000 cm^{-1}, and 1987 cm^{-1}. The comparison of the reflux progression shows the overall peak pattern shifting towards the growth of the 1987cm-1 peak. Thus, this specific peak became of

interest was the formation of the 1987cm^{-1} peak, as this peak pattern and intensity is only seen at maximum reflux time and at high temperatures.

By monitoring the reaction through IR, a distinct change can be seen when cooling the reaction mixture, indicating a further change of product (Figure R.5). The data shows that the product at high temperature (maximum time of reflux, top spectrum) has IR absorption peaks at lower frequencies than that of the cooled product (middle and bottom spectra), as the wavenumbers increase when cooled. Peaks of the high temperature product, 2078 cm^{-1} and 2000 cm^{-1} disappear while the 1987 cm^{-1} peak decreased in intensity; where in the cooled product, the 2092 cm^{-1}, 2004 cm^{-1}, and 1994 cm^{-1} peaks appear, as the 2052 cm^{-1} peak grew in intensity. The process of cooling the high temperature product to room temperature and evaluating the product stability in different solvents, acetonitrile (middle) and dichloromethane (bottom).

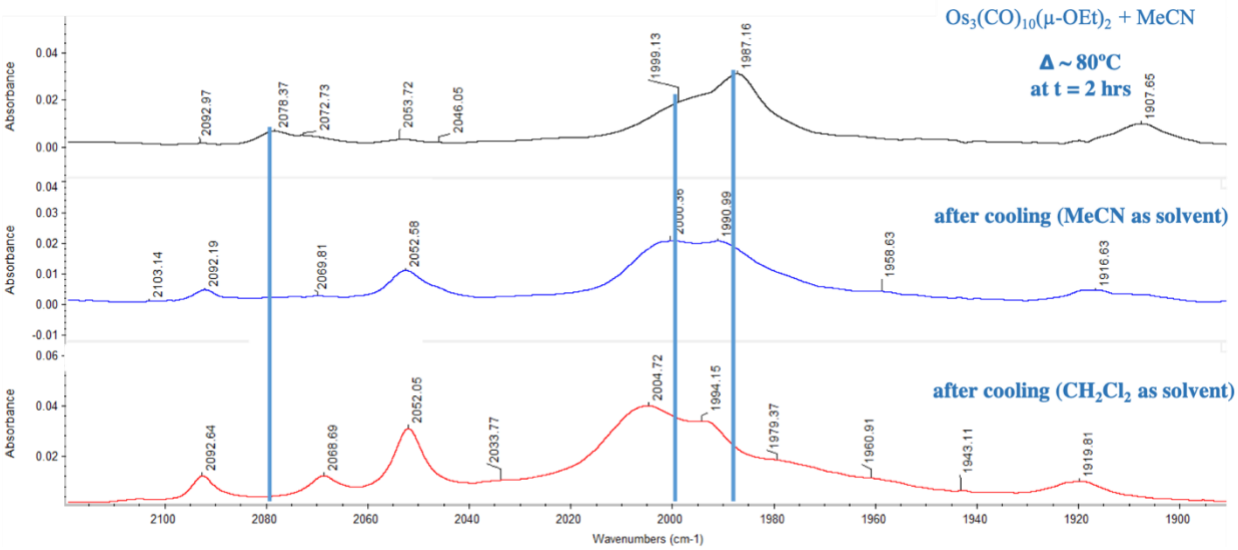

Figure R.5. Stacked infrared spectra demonstrating peak changes over reaction time: Spectrum at maximum reflux (t = 2hrs, top), when cooled, in acetonitrile (middle) and in dichloromethane (bottom). Measured in absorbance.

The solvent acetonitrile was removed and the solid product was dissolved in dichloromethane, to get a clearer IR spectrum, and to test the stability of the activated complex in

a not coordinated solvent. When in dichloromethane, slight shifts in the peak frequencies occurred in comparison to the product in acetonitrile (Figure R.5). Though slight shifts in frequency occurred (which is expected from differing solvents), the peaks retained the same general peak pattern from acetonitrile to dichloromethane. The retention of peak pattern indicates that the product is stable and does not change in dichloromethane.

Overall from the IR data, it can be deduced that the reaction led to an acetonitrile substituted product, due to the changes in peaks from starting to final - of which this compound has the formula $Os_3(CO)_{10-x}(\mu\text{-}OEt)_2(MeCN)_x$ (x being the number of coordinated acetonitrile ligands) (Figure R.7).

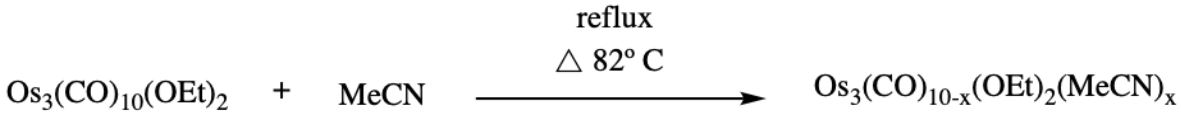

Figure R.7. Reaction scheme proposing substitution of 'x' acetonitrile ligand(s), replacing 'x' amount of carbonyl ligands of bisethoxide.

The IR data indicates that at higher temperatures, a higher level of substitution is occurring due to this lower frequency being observed; thus leading us to believe that the higher temperature product is disubstituted with acetonitrile ligands. The higher level of substitution correlating to lower frequencies is explained by when a carbonyl ligand being replaced by the second acetonitrile ligand, each CO ligand in the disubstituted product would experience more back donation from the attached osmium core, as there are less CO ligands to disperse electron density to (Figure R.6). So, more electrons from osmium will be donated to the π^* anti-bonding orbital of the CO ligand causing lower peak frequencies in the IR. The lower frequency arising from a higher level of substitution can also be attributed to acetonitrile being a σ-donor, where it does not compete for pi-e^- density.

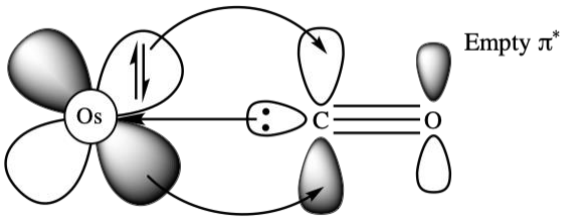

Figure R.6. Diagram illustrating back-donation from the osmium's d-orbital to the antibonding pi*-orbital of the carbonyl ligand. The carbon of the carbonyl is also participating in sigma-donation, as electrons are being donated to the osmium core.

When trying to characterize what the obtained product was, past IR spectra of osmium complexes with a substitution of an acetonitrile ligand were looked into. The experimental IR data of the proposed $Os_3(CO)_{10-x}(\mu\text{-}OEt)_2(MeCN)_x$ product (Figure R.8a) when the product is cooled is very similar to the known spectrum of $Os_3(CO)_9(\mu\text{-}OEt)_2(MeCN)$, synthesized by former Pearsall lab research student Shannon Higgins - where $Os_3(CO)_9(\mu\text{-}OEt)_2(MeCN)$ was synthesized using the $MeCN/Me_3NO$ synthesis approach (Figure R.8B)[18].

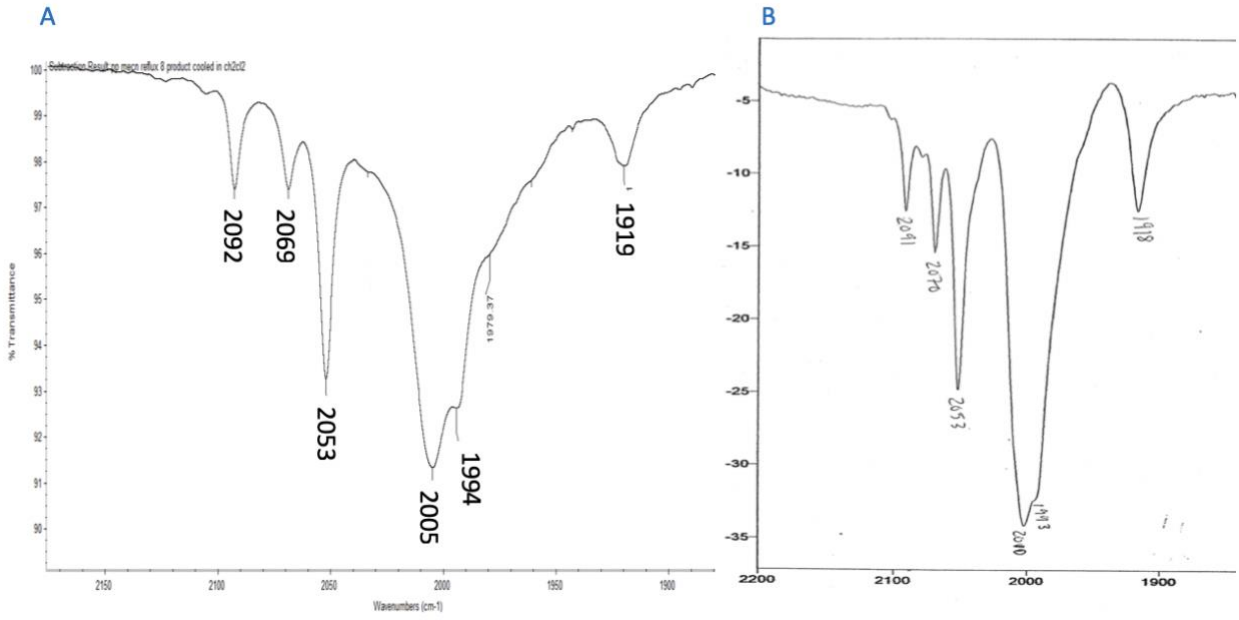

Figure R.8(A,B). Infrared spectrum comparison of (A) experimental reflux product ($Os_3(CO)_{10-x}(\mu\text{-}OEt)_2(MeCN)_x$) cooled in CH_2Cl_2 to (B) known spectrum of $Os_3(CO)_9(\mu\text{-}OEt)_2(MeCN)$ obtained by Shannon Higgins[18]. Measured in transmittance.

Notable peaks of $Os_3(CO)_9(\mu\text{-}OEt)_2(MeCN)$ (Figure R.8B) are $2091cm^{-1}$, $2070cm^{-1}$, $2053cm^{-1}$, $2010cm^{-1}$, $1993cm^{-1}$, and $1918cm^{-1}$. These peaks are similar to the peaks of the experimental acetonitrile product - which leads to the proposal that the direct reaction of $Os_3(CO)_{10}(\mu\text{-}OEt)_2$ in acetonitrile ultimately leads to $Os_3(CO)_9(\mu\text{-}OEt)_2(MeCN)$.

To revisit the observable changes in IR spectra that are seen at high to room temperatures, not only did the wavelengths of peaks change, but so did the intensity of peaks present (Figure R.5). As we can deduce that the product seen at room temperature is $Os_3(CO)_9(\mu\text{-}OEt)_2(MeCN)$, the product at high temperatures likely possesses more substitution due to the higher frequencies. When comparing the spectra the IR spectra observed at room temperature (in MeCN and CH_2Cl_2) decreased in intensity in comparison to the product at high temperatures (Figure R.5). This further supports product change from high to low temperature, as a decrease in intensity is consistent with the reaction scavenging for CO. Thus, it data gives more reason to deduce that the high temperature product is the disubstituted product, $Os_3(CO)_8(\mu\text{-}OEt)_2(MeCN)_2$, which decomposes upon cooling the product to room temperature, further resulting in the product $Os_3(CO)_9(\mu\text{-}OEt)_2(MeCN)$ and acetonitrile.

To further confirm this deduction of the ultimate product being $Os_3(CO)_9(\mu\text{-}OEt)_2(MeCN)$, ^1H NMR spectra were taken of the product, one immediately after synthesis, and another approximately 36 hours later to characterize the number of hydrogens in the acetonitrile ligand(s) attached to the osmium core, in relation to the bridging ethoxides.

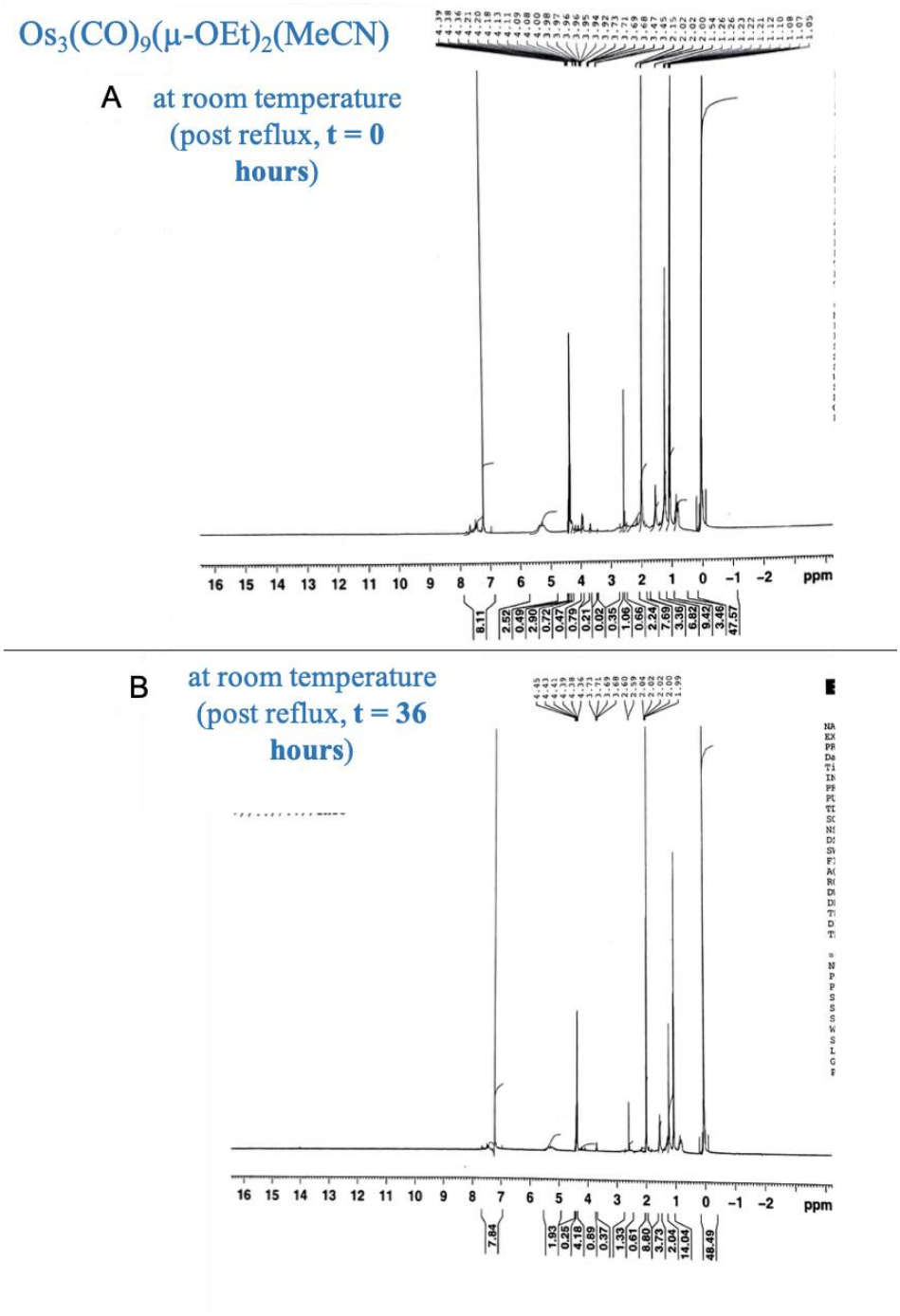

Figure R.9(A,B) Full ^{1}H NMR spectra comparison of proposed product $Os_3(CO)_9(\mu\text{-}OEt)_2(MeCN)$ at initial reaction time (top) and after 36 hours (bottom).

A region of chemical shift that showed difference between the two spectra was from ~3.9-4.0 ppm. This was closer examined to see peak difference (Figure R.10).

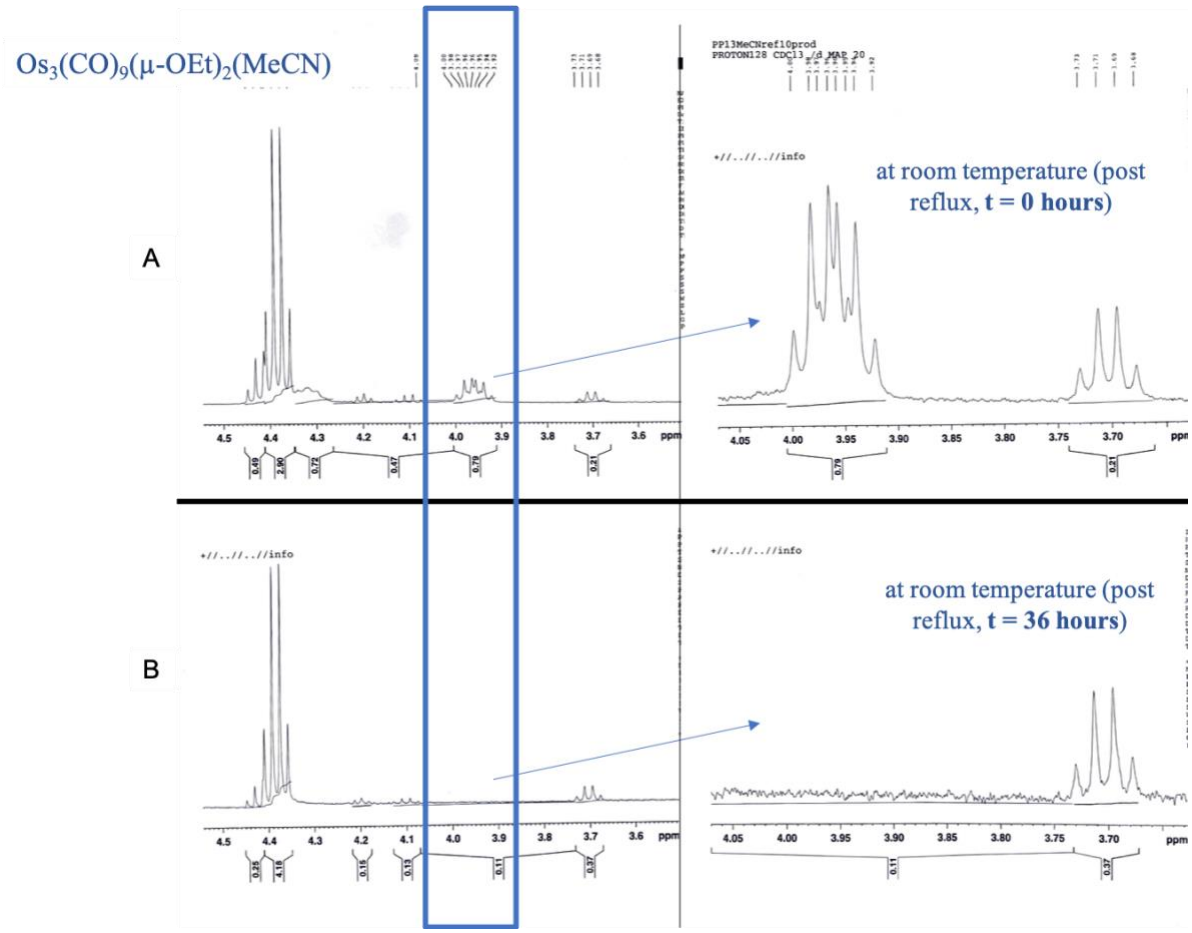

Figure R.10(A,B). Closer examination of peak pattern of ^{1}H NMR spectra observed of product initially (A) and after 36 hours (B).

A series of overlapping multiplets at ~3.9-4.0 seen in A (right) can be assigned to the -CH_2 group of the ethoxide ligands. These overlapping multiplets indicate that the coordinated acetonitrile ligand is trans to an ethoxide ligand instead of being trans to the Os-Os bond (would not be seen as overlapping multiplets if trans to the Os-Os bond). One multiplet is shifted more downfield than the other multiplet due to the acetonitrile being trans to only one of the bridging ethoxides, while the other ethoxide is trans to a carbonyl ligand; thus creating different chemical shifts (Figure R.11). Over the span of the 36 hours, this overlapping multiplet disappears, indicating there is no more coordinated acetonitrile in the product. The other set of multiplets

found at ~4.35-4.45ppm can also be assigned to the -CH_2- groups of bisethoxide. A triplet at ~1.1 ppm in both spectra can be assigned to the -CH_3 groups of bisethoxide. The disappearance of the multiplets at ~4ppm seen after 36 hours correspond to the decomposition of the product. After 36 hours, IR analysis was also obtained and peaks resembled those signature to bisethoxide only. An unidentifiable peak is present at ~2.6ppm in both spectra. The coordinated acetonitrile ligand peak is not seen in the spectrum, but is reported to appear at approximately 2.28ppm[4].

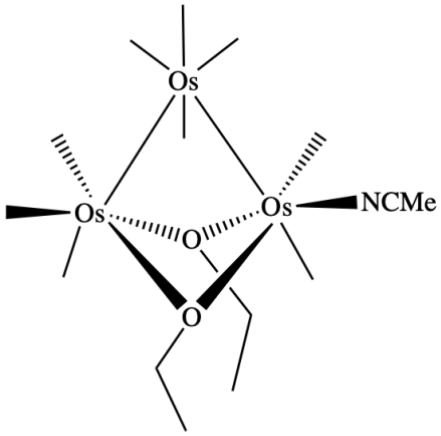

*All other bonds to Os are CO

Figure R.11. Structural representation of product $Os_3(CO)_9(\mu\text{-}OEt)_2(MeCN)$ with stereochemical positioning of the coordinated acetonitrile ligand, seen trans to the bridging ethoxide.

To further analyze how many acetonitrile ligands are coordinated to our product, a ratio between the bridging ethoxide ligands and the coordinated acetonitrile ligand peaks must be made. According to prior research done by Pearsall, it was found to be a 2:1 ratio; two ethoxides per one acetonitrile ligand[4]. For this research, a ratio could not be obtained due to the lack of the coordinated acetonitrile ligand peak. It can be confirmed that acetonitrile was coordinated to the osmium complex by IR, which was obtained prior to the NMR spectrum.

ii. Reaction of $Os_3(CO)_9(\mu\text{-}OEt)_2(MeCN)$ in trimethylphosphite, $P(OMe)_3$

To further confirm the formation of the product $Os_3(CO)_9(\mu\text{-}OEt)_2(MeCN)$, alternate routes were explored to confirm ligand substitution. Previous research has studied the substitution of trimethylphosphite, P(OMe)3, ligands for NCMe ligands[4]. In specific, the reaction of $Os_3(CO)_9(\mu\text{-}OEt)_2(MeCN)$ with one equivalent of $P(OMe)_3$ together at room temperature resulted in the product $Os_3(CO)_9(\mu\text{-}OEt)_2(P(OMe)_3)$ (Figure R.12).

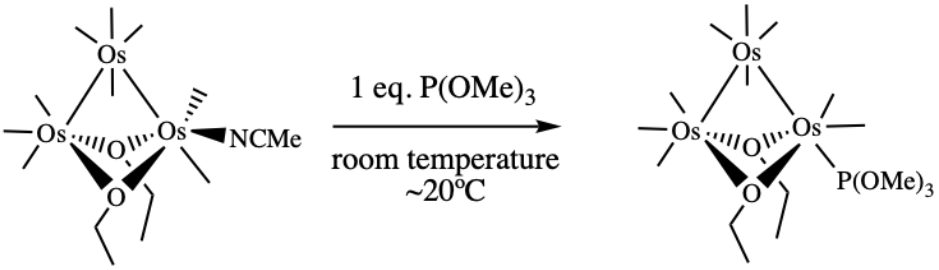

Figure R.12. Reaction scheme of $Os_3(CO)_9(\mu\text{-}OEt)_2(NCMe)$ with $P(OMe)_3$.

This is significant since at higher temperatures, the disubstituted product $Os_3(CO)_8(\mu\text{-}OEt)_2(P(OMe)_3)_2$ is known to form, as the $P(OMe)_3$ ligand readily replaces either a coordinated carbonyl or acetonitrile ligand (Figure R.13)[4].

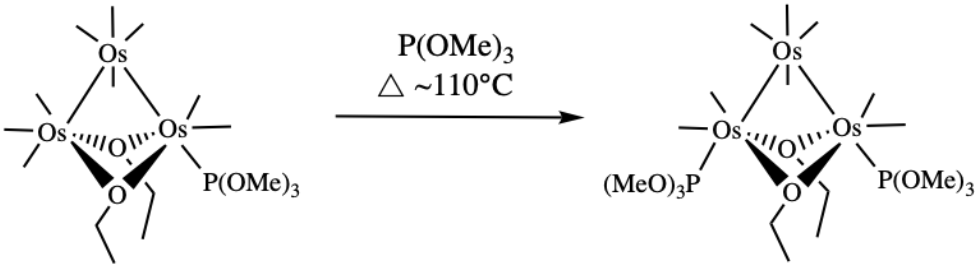

Figure R.13. Reaction scheme of $Os_3(CO)_9(\mu\text{-}OEt)_2(P(OMe)_3)$ refluxed in $P(OMe)_3$.

In addition, a mixture of bisethoxide and $P(OMe)_3$ at room temperature yielded no reaction over two weeks, as all signature peaks of bisethoxide remained and peak pattern did not change. By $P(OMe)_3$ not substituting the CO ligands of bisethoxide at room temperature, it

shows that $P(OMe)_3$ will either only substitute for acetonitrile at room temperature, or a carbonyl ligand with heat. Thus, by conducting the reaction of $P(OMe)_3$ at room temperature to our synthesized acetonitrile complex, it can be assumed that only replacement of coordinated acetonitrile ligand(s) will occur since acetonitrile is a weaker ligand than $P(OMe)_3$. The principle of direct ligand substitution is seen to obtain a monosubstituted $P(OMe)_3$ product to confirm the acetonitrile synthetic product.

These multitudes of reactions can be compiled into one cohesive story, as each reaction supports one another by giving background on temperature, reagents, starting material, and obtained product. To summarize, $P(OMe)_3$ was added at room temperature to the believed synthesized product, $Os_3(CO)_9(\mu\text{-}OEt)_2(NCMe)$, to ensure there is an acetonitrile ligand coordinated. If substitution of the ligand occurs at room temperature, there must have been an acetonitrile ligand coordinated. This walkthrough can be seen in Figure R.14, to show the relationship of each reaction and how they all connect to help support the classification of the product without using NMR data.

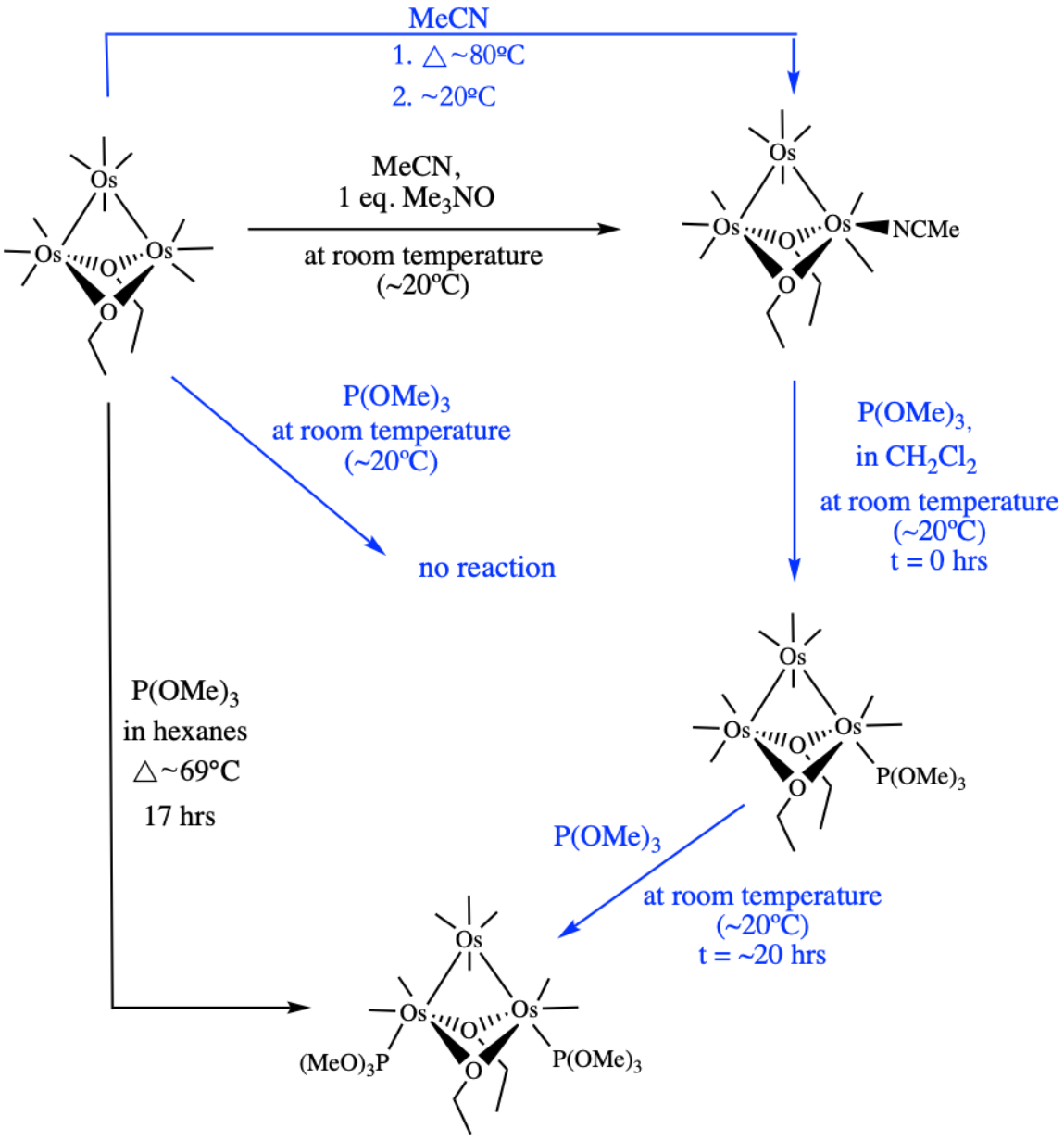

Figure R.14. Compilation of reaction schemes to confirm formation of the product $Os_3(CO)_9(\mu\text{-}OEt)_2(MeCN)$ through known products of other syntheses[4]. Emphasized in blue are the reactions I conducted to classify the product $Os_3(CO)_9(\mu\text{-}OEt)_2(MeCN)$ through the direct reflux of bisethoxide in acetonitrile.

To test this logic and to further confirm the formation of the monosubstituted product $Os_3(CO)_9(\mu\text{-}OEt)_2(MeCN)$, trimethylphosphite ($P(OMe)_3$) was added to the acetonitrile product in dichloromethane and stirred at room temperature.

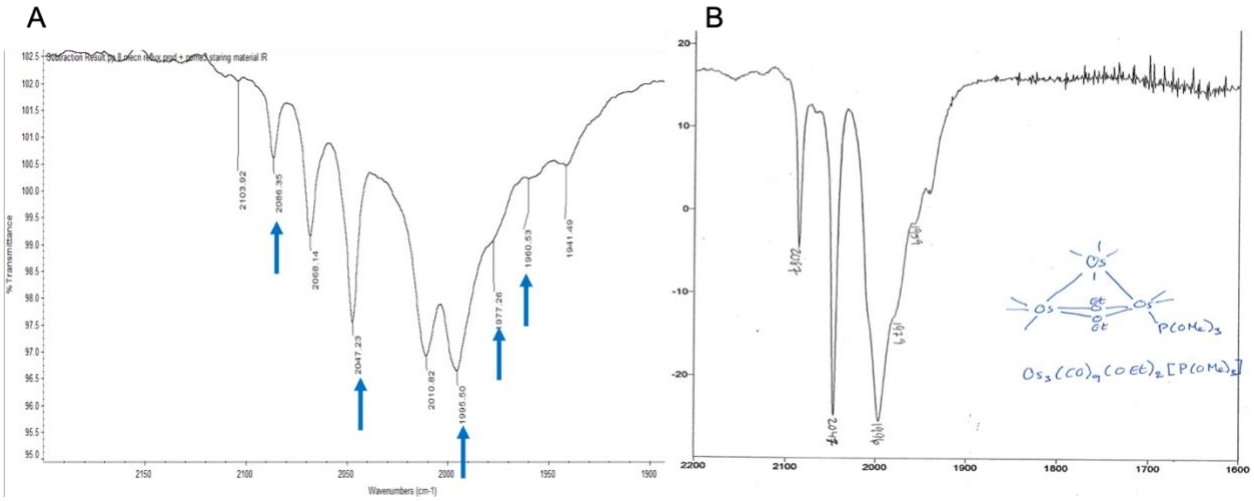

Figure R.15(A,B). Infrared spectra of (A) $Os_3(CO)_9(\mu\text{-}OEt)_2(MeCN)$ cooled after reflux with $P(OMe)_3$ initially added, (in CH_2Cl_2); and (B) reference IR spectrum of $Os_3(CO)_9(\mu\text{-}OEt)_2(P(OMe)_3)$, conducted by Shannon Higgins[19]. Measured in transmittance.

Upon the addition of $P(OMe)_3$ to the acetonitrile product, differences in peaks have already begun to appear (Figure R.15). Most noticeably, the 2004cm^{-1} peak of the MeCN complex disappeared while a peak of 2010cm^{-1} appeared, while the 1994cm^{-1} peak of the MeCN complex decreased in intensity when present in the $P(OMe)_3$ complex. The 2052cm^{-1} and 2092cm^{-1}peak of the MeCN complex disappeared while peaks at 2047cm^{-1} and 2086cm-1 appeared in the $P(OMe)_3$ complex. Additional peaks present in the spectrum are thought to correspond to peaks of bisethoxide (peaks 2103cm^{-1}, 2068cm^{-1}, and potentially the 2010cm^{-1}). With the initial addition of the $P(OMe)_3$, the IR spectrum has all five characteristic known peaks of $Os_3(CO)_9(\mu\text{-}OEt)_2(P(OMe)_3)$ - such as the 2086cm^{-1}, 2047cm^{-1}, 1996cm^{-1}, 1977cm^{-1}, and the 1960cm^{-1} (observed in reference spectrum in Figure R.15B). These peaks are highlighted in blue,

in Figure R.15. This allows us to deduce that the compound formed the product $Os_3(CO)_9(\mu\text{-}OEt)_2(P(OMe)_3)$ upon addition of $P(OMe)_3$ – thus proving that the final product is $Os_3(CO)_9(\mu\text{-}OEt)_2(MeCN)$.

When the reaction was left overnight, and the progress was checked approximately 20 hours later by IR, a different spectrum was obtained than observed upon initial addition, suggesting a different product forming. In each trial, IR spectra taken after this amount of time yielded results with peaks similar to the known peaks in the disubstituted complex, $Os_3(CO)_8(\mu\text{-}OEt)_2(P(OMe)_3)_2$ (Figure R.16A).

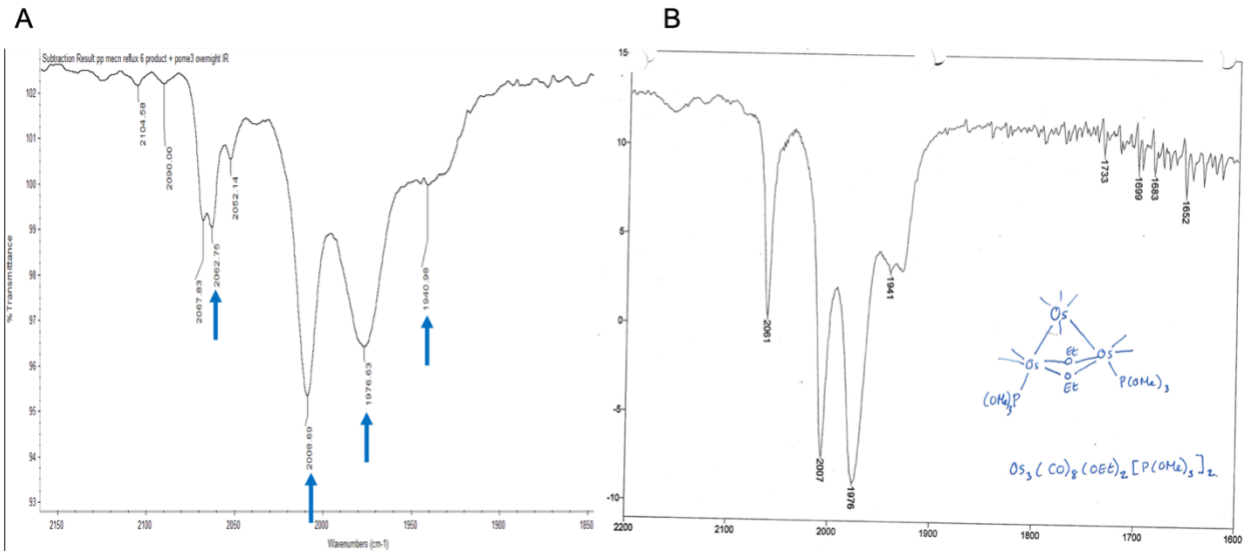

Figure R.16(A,B). Infrared spectra of (A) $Os_3(CO)_{10\text{-}x}(\mu\text{-}OEt)_2(P(OMe)_3)_x$ product obtained, and (B) reference IR spectrum of $Os_3(CO)_8(\mu\text{-}OEt)_2(P(OMe)_3)_2$, conducted by Shannon Higgins[19]. Measured in transmittance.

These peaks and pattern of $2062cm^{-1}$, $2008cm^{-1}$, $1976cm^{-1}$, and $1940cm^{-1}$ resemble peaks of the known $Os_3(CO)_8(\mu\text{-}OEt)_2(P(OMe)_3)_2$ complex, highlighted in blue in Figure R.16A. We propose that when left to progress over time in dichloromethane and unreacted $P(OMe)_3$, the disubstituted $(CO)_8(P(OMe)_3)_2$ complex formed. The formation of the disubstituted $P(OMe)_3$ product from $Os(CO)_9(\mu\text{-}OH)_2(P(OMe)_3)$ has been observed by prior Pearsall lab member David

Moore, so forming $Os_3(CO)_8(\mu\text{-}OEt)_2(P(OMe)_3)_2$ from the $(CO)_9(P(OMe)_3)$ complex is supported[20].

This hypothesis of the monosubstituted product transforming into the disubstituted product over time has led us into deeper investigation of this part of the synthesis. When the acetonitrile reflux product was isolated and dissolved in dichloromethane, a drop of $P(OMe)_3$ was added and stirred at room temperature (same parameters as prior trials with $P(OMe)_3$). The reaction was monitored periodically instead of leaving it overnight. IRs were taken over a time span of approximately 20 hours.

When the $P(OMe)_3$ was added, those peaks were recorded. Each IR after the initial was compared to the initial to see any peak changes - appearances, disappearances, or intensity changes that may occur in the reaction (Figure R.17).

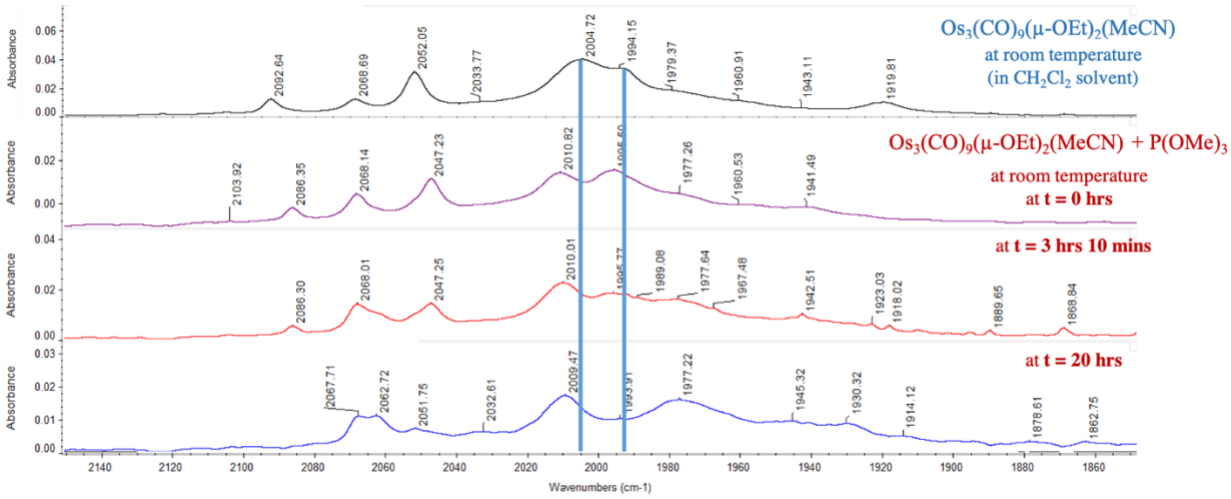

Figure R.17. Stacked IR spectra showing reaction progression of the addition of $P(OMe)_3$ to $Os_3(CO)_9(\mu\text{-}OEt)_2(MeCN)$. Order of spectrum: before the addition of $P(OMe)_3$ (top); initial time when $P(OMe)_3$ is added (2nd); addition of $P(OMe)_3$ reaction after 3hr 10 min of (3rd); and reaction after ~20 hrs (bottom). Measured in absorbance.

Figure R.17 features a stacked spectrum layout of different time points during the reaction progression. Spectral peak changes during the reaction can be visualized through the

differences in peak wavelengths from the blue line, comparing new peaks to the peaks of the acetonitrile complex (Figure R.17). The 2092 cm^{-1}, 2052 cm-1, 2004 cm^{-1}, and 1994 cm^{-1} peaks of the MeCN complex disappear while peaks at 2086 cm^{-1}, 2047 cm^{-1}, 2010 cm^{-1}, and 1995 cm^{-1} appear upon initial addition of $P(OMe)_3$. Over the 20 hours observed, these peaks decrease in intensity, while new peaks at 2062 cm^{-1}, 2051 cm^{-1}, 2009 cm^{-1}, and 1977 cm^{-1} increase.

Specifically, peaks at 2010cm^{-1}, 1995cm^{-1}, and 1979 cm^{-1} of the reaction over time are examined closer (Figure R.18).

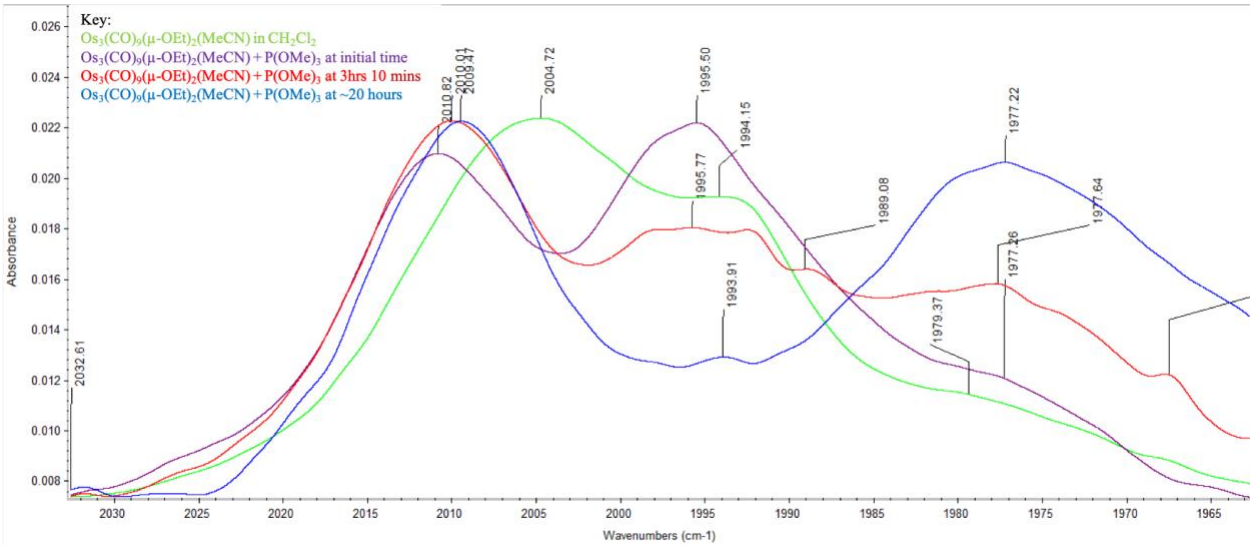

Figure R.18. Overlay spectral analysis, focusing on the peak region ~2035 – 1960 cm^{-1} containing peaks of interest - 2010cm^{-1}, 1995cm^{-1}, and 1979 cm^{-1}. Measured in absorbance.

In comparing the spectra with $P(OMe)_3$ added, all the peaks shift lower in wavelength, indicating that a higher level of substitution occurred over time. The 1995cm^{-1} peak is depleting as the reaction progresses, while the 1977cm^{-1} peak is growing in. The 1995cm^{-1} peak is characteristic to the monosubstituted $P(OMe)_3$ product and the 1977cm^{-1} is only characteristic to the disubstituted product. The reaction looked at after approximately 20 hours possesses peaks characteristic to the disubstituted $P(OMe)_3$ product, and other peaks characteristic to bisethoxide.

Thus, these results show that with the addition of $P(OMe)_3$ to $Os_3(CO)_9(\mu\text{-}OEt)_2(MeCN)$ at room temperature, the monosubstituted $P(OMe)_3$ product, $Os_3(CO)_9(\mu\text{-}OEt)_2(P(OMe)_3)$ is obtained initially and then it converts to the disubstituted product, $Os_3(CO)_8(\mu\text{-}OEt)_2(P(OMe)_3)_2$ over time (Figure R.19).

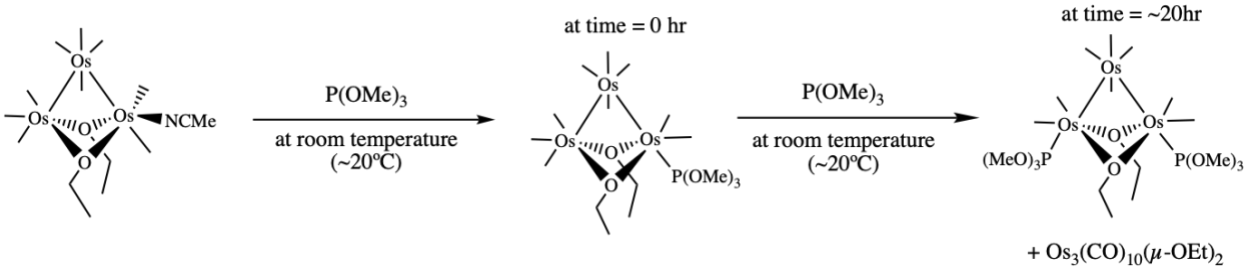

Figure R.19. Reaction scheme of the addition of $P(OMe)_3$ to $Os_3(CO)_9(\mu\text{-}OEt)_2(MeCN)$, at room temperature, over ~20 hours.

iii. Reaction of $Os_3(CO)_9(\mu\text{-}OEt)_2(MeCN)$ in triphenylphosphine, PPh_3

Since we deduced that the monosubstituted $P(OMe)_3$ product converts to the disubstituted $P(OMe)_3$ product when left overnight, a different ligand, using triphenylphosphine (PPh_3) became of interest. PPh_3 is a bulkier ligand than $P(OMe)_3$, so it was proposed that it may potentially not progress past the monosubstituted ligand product like with the $P(OMe)_3$ when left overnight.

To test this, the acetonitrile reflux product was dissolved in dichloromethane, and an excess of PPh_3 was added to the reaction mixture. The reaction of the initial addition of PPh_3 was monitored by IR (Figure R.20).

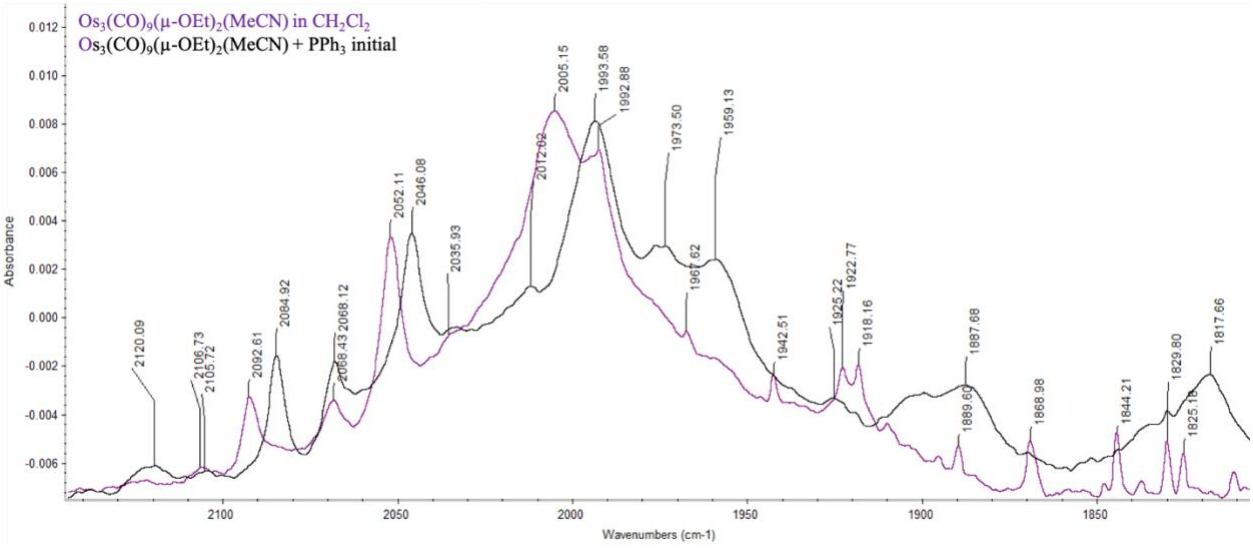

Figure R.20. Infrared spectrum of the initial reaction between $Os_3(CO)_9(\mu\text{-}OEt)_2(MeCN)$ and PPh_3, dissolved in dichloromethane, stirring at room temperature (black) compared to the IR of $Os_3(CO)_9(\mu\text{-}OEt)_2(MeCN)$ in dichloromethane (purple). Measured in absorbance.

When PPh_3 is added, there are some observable peak differences. The strong ~2005cm^{-1} peak of the acetonitrile complex decreases intensity to a small shoulder peak at 2012cm^{-1}, while the 1993 cm^{-1} peak of the acetonitrile complex grows in once PPh_3 was added. Other smaller peaks shift slightly in wavenumber, but these identified peaks are also changing intensity and overall pattern. The spectrum of the reaction mixture upon initial addition of PPh_3 was unclear (very noisy) and did not distinguishably match any reference spectra available.

The reaction of PPh_3 and the acetonitrile complex stirred for a week and noticeable change in the IR was observed (Figure R.21).

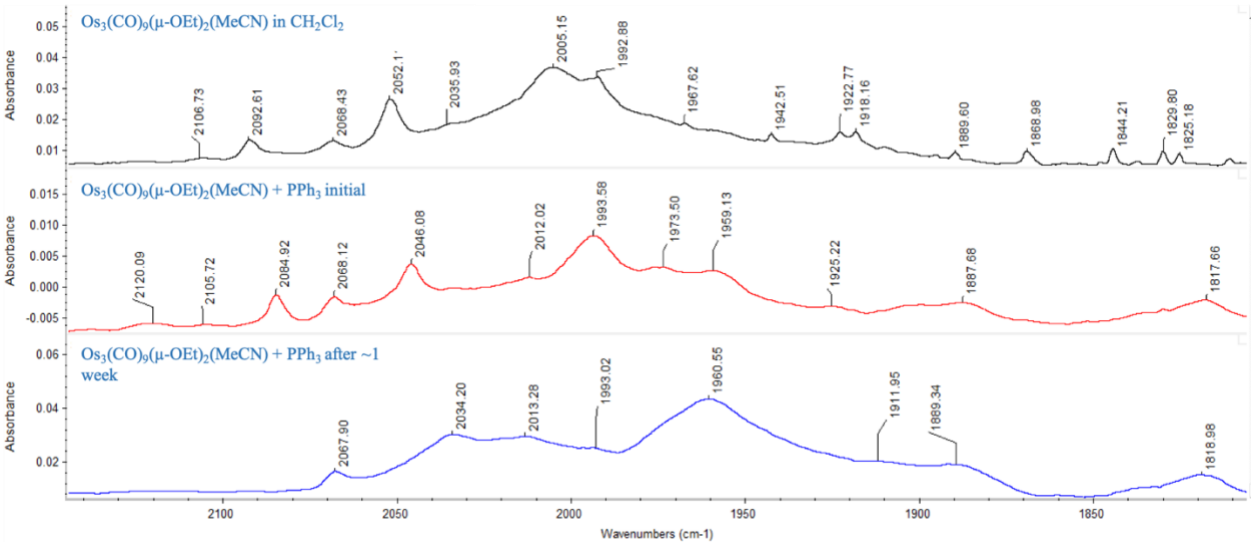

Figure R.21. Stacked spectral analysis of the reaction $Os_3(CO)_9(\mu\text{-}OEt)_2(MeCN)$ with PPh_3. Measured in absorbance.

Though changes in the IR spectra occur over the span of seven days, the spectrum obtained for after seven days of reacting (bottom spectrum, Figure R.21), the IR shows no recognizable osmium carbonyl products.

A TLC was obtained comparing the PPh_3 synthesis product to solid PPh_3 dissolved in dichloromethane (Figure R.22).

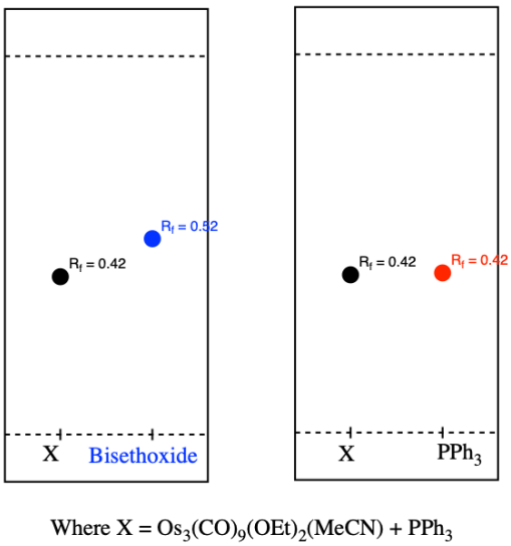

Figure R.22. A TLC of ($Os_3(CO)_9(\mu\text{-}OEt)_2(MeCN)$ + PPh_3) compared to bisethoxide (left); and a TLC of the acetonitrile complex and PPh_3 reaction mixture compared to PPh_3 (right).

The TLC was inconclusive since it may be obscured by PPh_3, as the Rf value of the proposed PPh_3 product matches the Rf value of the solid PPh_3 reagent (Figure R.20). As there are no recognizable substituted products in the IR spectra collected, the results of the substitution of PPh_3 with $Os_3(CO)_9(\mu\text{-}OEt)_2(MeCN)$ are inconclusive. More experimental results and repeat trials are needed to make any conclusions with the PPh_3 ligand and the acetonitrile complex's interactions.

6. Conclusion and Future Directions

Through this research, we have successfully synthesized an acetonitrile-substituted triosmium cluster through a different synthetic approach, where this complex has demonstrated that it is likely to be $Os_3(CO)_9(\mu\text{-}OEt)_2(NCMe)$. Previous attempts of creating an acetonitrile substituted product utilized the reagent Me_3NO as an aid for ligand substitution; but Me_3NO was not used in this work[4]. Through the direct reaction of bisethoxide in acetonitrile at reflux temperature of 80ºC, we had anticipated the formation of the $Os_3(CO)_8(\mu\text{-}OEt)_2(NCMe)_2$ complex as our end product. Through IR analysis, it is likely that at high temperatures, we see the disubstituted product $Os_3(CO)_8(\mu\text{-}OEt)_2(NCMe)_2$, and when this product is cooled to room temperature, the monosubstituted product $Os_3(CO)_9(\mu\text{-}OEt)_2(NCMe)$ is formed (Figure F.1).

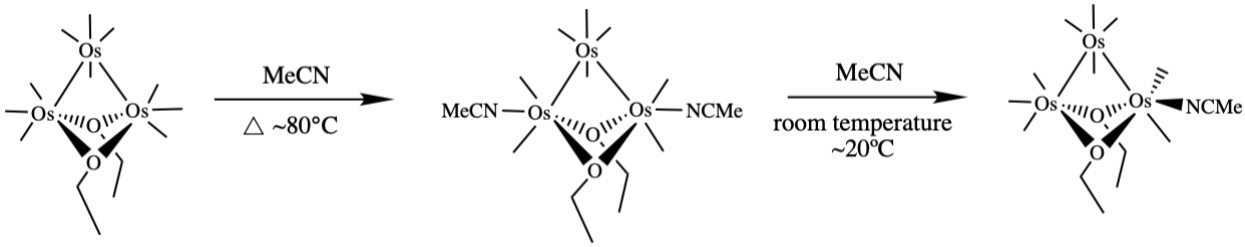

Figure F.1. Reaction scheme of products obtained through bisethoxide in acetonitrile at reflux and room temperatures.

Through IR and ^1H NMR analysis, it was concluded that the ultimate product of $Os_3(CO)_9(\mu\text{-}OEt)_2(NCMe)$ decomposed to $Os_3(CO)_{10}(\mu\text{-}OEt)_2$ in approximately 36 hours. Thus, the stability of the complex through this synthetic route may not be the most practical synthetic approach.

Further investigation and research is needed to draw further conclusions about the acetonitrile product formed at high temperature – to see if it is in fact the disubstituted acetonitrile product, or another acetonitrile intermediate (potentially an isomer of the monosubstituted acetonitrile product). In addition, the stability of the product and acetonitrile as

a ligand is also in question - as the product decomposes shortly after production, and the creation of a disubstituted acetonitrile complex does not seem to be favorable as it seems to be only stable at high temperatures.

Due to the decomposition of $Os_3(CO)_9(\mu\text{-}OEt)_2(MeCN)$ shortly after synthesis, there was no biological assessment as it was not stable. The solubility of synthesized complexes in polar solvents (water, acetonitrile, ethanol) need to be tested in the future if the product remains stable enough. In the future, it would be beneficial to look into ways in optimizing the synthesized product's life, and potentially slowing down the decomposition of $Os_3(CO)_9(\mu\text{-}OEt)_2(MeCN)$ so its solubility and biological applications can be analyzed. Reaction conditions and procedure may be factors that need to be reevaluated in order maximize product life, to limit any interaction that the product may have with air or contaminants. Actions could include such things as reducing or controlling moments where the reaction mixture is not in a nitrogenous controlled environment (in between evaporations, adding reagents, taking IRs/TLCs) more; if syntheses need utilize a glove box or Schlenk line; or if glassware need to be vacuum purged and filled with nitrogen gas before conducting a synthesis. Therefore, future research leads us in the direction of trying to come up with a standard method to successfully produce the disubstituted compound, $Os_3(CO)_8(\mu\text{-}OEt)_2(MeCN)_2$, and monosubstituted complex $Os_3(CO)_9(\mu\text{-}OEt)_2(MeCN)$ as both are complexes with biological interest worth investigating.

Another direction in the future would be to synthesize other biologically interesting osmium carbonyl complexes with acetonitrile coordinated. As the Pearsall lab has shown via various synthesis reactions, bisethoxide forms a diosmium unit when reacted with an amide or carboxylate compound. Based on the structure of known transition metal complexes that possess biological activity, such as the dirhodium complexes, it would be interesting to look into the

synthesis of a diosmium unit with acetonitrile ligands coordinated. To do this in the future, one would reflux bisethoxide in acetic acid to first produce a diosmium carboxylate complex (Figure F.2).

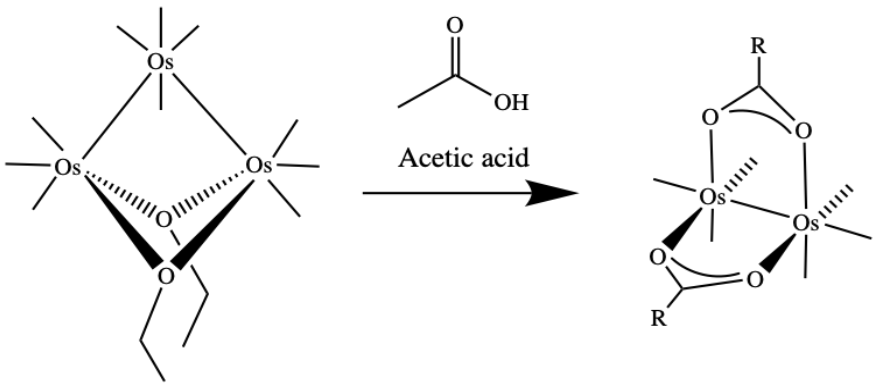

Figure F.2. Reaction of bisethoxide in acetic acid to yield known diosmium complex (where R = CH_3).

This diosmium complex will then be refluxed in acetonitrile to potentially produce a complex with axial acetonitrile ligands (Figure F.3).

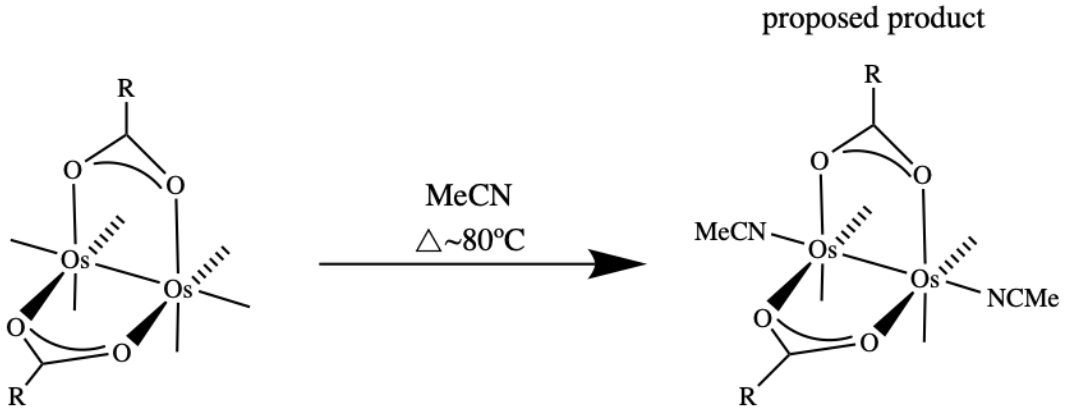

Figure F.3. Reaction of the diosmium complex $Os_2(CO)_6(CH_3COO)_2$ and acetonitrile to yield possible product (where R = CH_3).

Similarities in structure to Dunham's dirhodium complexes, in combination to proven biological activity of osmium carbonyl clusters by Leong et al., provide belief that diosmium carboxylate and amide complexes with coordinated acetonitrile ligands are compounds of biological interest.

Along with synthesizing additional biologically interesting osmium carbonyl complexes, The characterization of the product $Os_3(CO)_9(\mu\text{-}OEt)_2(MeCN)$ gives promise for the future in hopes of successfully characterizing the disubstituted acetonitrile complex, $Os_3(CO)_8(\mu\text{-}OEt)_2(MeCN)_2$, in later research to follow, as acetonitrile substituted osmium carbonyl complexes are chemically and biologically interesting to investigate further.

7. Discovery and Synthetic Routes of $Os_3(CO)_{10}(\mu\text{-}OEt)_2$– a Review

The simplest way to form bisethoxide was discovered in 1968 and is by a reaction of osmium tetroxide (OsO_4) with carbon monoxide in ethanol, which produces triosmium dodecacarbonyl ($Os_3(CO)_{12}$) and a byproduct of bisethoxide ($Os_3(CO)_{10}(\mu\text{-}OEt)_2$)[21]. This reaction also produced a side product of CO_2 gas (Figure D.1). The issues with this reaction are that osmium tetroxide is toxic and that the reaction only produced less than five percent yield of bisethoxide because it is a byproduct of the reaction. Because of these issues, other routes had to be explored.

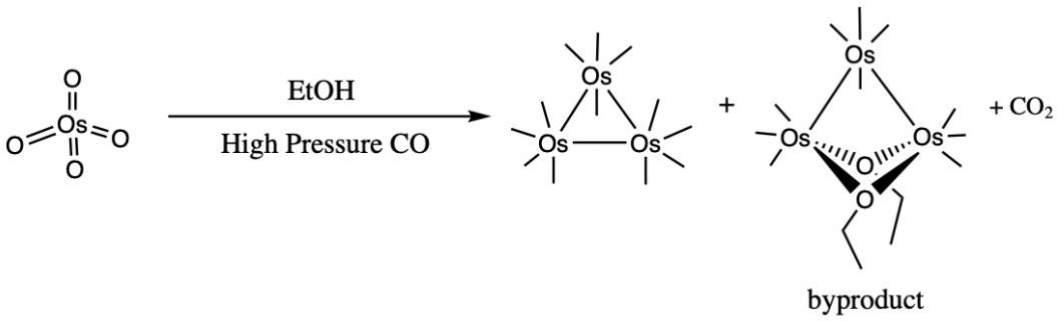

Figure D.1. Osmium tetroxide reaction yielding triosmium dodecacarbonyl and byproduct of bisethoxide.

In 1996, Pearsall lab student Stephanie Schlecht studied the synthesis of dihalo-bridged clusters, which the starting point of this synthesis was $Os_3(CO)_{12}$[22]. In her research, she produced and isolated a linear chlorine-osmium complex, $Os_3(CO)_{12}(Cl)_2$, by reacting triosmium dodecacarbonyl with bubbled Cl_2 gas, refluxed with cyclohexane. The linear chlorine-osmium complex product was isolated by bubbling nitrogen gas to displace unreacted chlorine, and the cyclohexane solvent was evaporated. In this, $Os_3(CO)_{12}$ opened up from a three Os-Os system into a linear two Os-Os system, with chlorines attached to the end osmiums to create the linear

product $Os_3(CO)_{12}(Cl)_2$. On the basis of known literature, she continued her research to isolate $Os_3(CO)_{10}(\mu\text{-}Cl)_2$; synthesized by reacting linear $Os_3(CO)_{12}(Cl)_2$ with toluene at reflux, to lose two carbonyl ligands (Figure D.2). Thus, showing $Os_3(CO)_{12}$ can produce dihalo-bridged clusters ($Os_3(CO)_{10}(\mu\text{-}X)_2$) through a linear halide intermediate $Os_3(CO)_{12}(X)_2$. The synthesis of $Os_3(CO)_{10}(\mu\text{-}X)_2$ provided a starting point for the synthesis of $Os_3(CO)_{10}(\mu\text{-}OR)_2$ clusters.

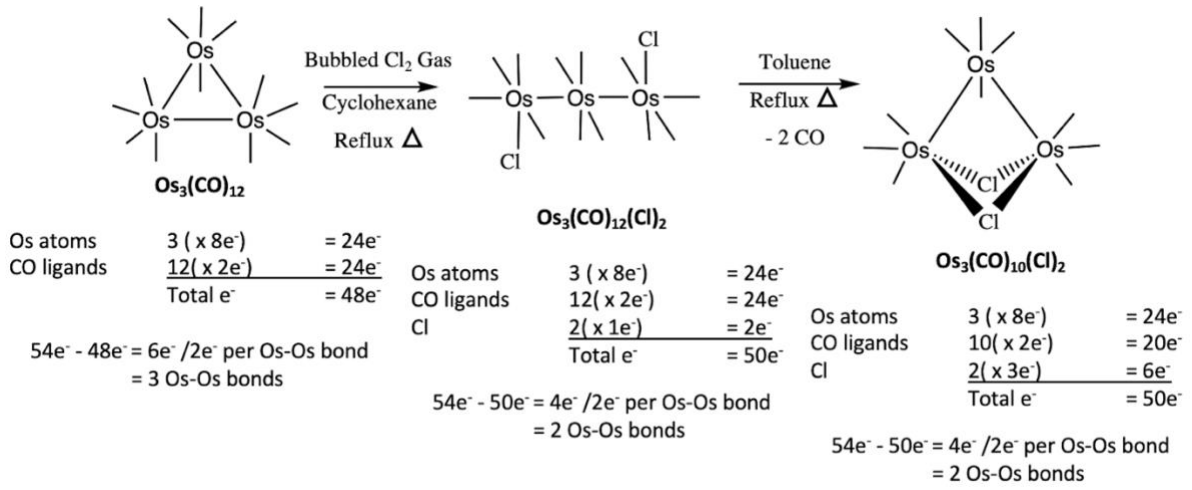

Figure D.2. Synthesis of $Os_3(CO)_{12}(Cl)_2$ and $Os_3(CO)_{10}(\mu\text{-}Cl)_2$ from $Os_3(CO)_{12}$, with 18-electron rule counts for each cluster. Chlorine goes from a $1e^-$ donor in the linear cluster to a $3e^-$ donor in the bridged cluster.

In 2010, Ashish Shah utilized Schlecht's research findings and proposed a route to create bisethoxide[23, 24]. The linear intermediate $Os_3(CO)_{12}(Cl)_2$ was reacted with ethanol at reflux to produce bisethoxide, $Os_3(CO)_{10}(\mu\text{-}OEt)_2$ (Figure D.3). This method showed promise with 75% yield of bisethoxide. However, using chlorine gas in undergraduate research is not favored due to its toxicity. Because of this, other halides were investigated.

In 2012, Erika Portero looked at linear complexes $Os_3(CO)_{12}(Br)_2$ and $Os_3(CO)_{12}(I)_2$ to react with ethanol at reflux to produce bisethoxide[25] (Figure D.3).

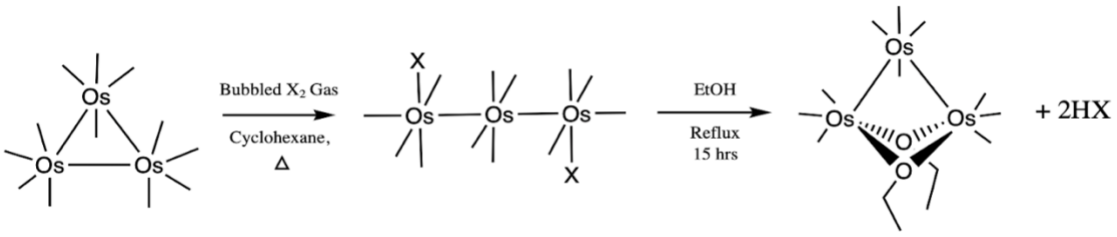

Figure D.3. Formation of bisethoxide by linear $Os_3(CO)_{12}(X)_2$, X = Cl, Br, or I.

The use of halogens bromine and iodine produced overall not great results: $Os_3(CO)_{12}(I)_2$ yielded no bisethoxide, and $Os_3(CO)_{12}(Br)_2$ yielded less than half the yield of bisethoxide obtained by using chlorine, in more than double the reaction time.

In 2014, Estephanie Rivero modified the Pearsall lab's bisethoxide synthesis route as she focused on a route that had a bridging halide intermediate, $Os_3(CO)_{10}(\mu\text{-}X)_2$, instead of linear halide intermediate[26]. This bridging halide intermediate with two less carbonyl ligands than the linear halide intermediate, $Os_3(CO)_{12}(X)_2$, was isolated in the reaction attempts of Shah and Portero. $Os_3(CO)_{10}(\mu\text{-}X)_2$ shows greater reactivity than $Os_3(CO)_{12}$ because it provides a more reactive center, as the third Os-Os bond found in triosmium dodecacarbonyl is replaced by the bridging reactive halides. When carrying out the reaction shown in Figure D.4, Rivero found that the reaction was reverting from bisethoxide back to the bridged halide configuration because of the presence of a strong acid as a product[26]. To drive the reaction forward and to neutralize the acid, the strong base alumina Al_2O_3 was added to the reaction to increase the yield of bisethoxide. With the addition of alumina to the reaction, the yields of bisethoxide from Cl, Br, and I were 54.7%, 39.8%, and 19.3%, respectively, showing that the reaction route using chlorine yielded the most amount of bisethoxide among the halides. The percent yields were not as high as expected even with the addition of alumina compared to the 75% yield of bisethoxide obtained in Shah's synthesis method[24]. However, yields were obtained for each halide through

this route, which was not evident in Portero's results using the linear halide intermediate, and so, this gave hope that the addition of alumina would aid future research as it sped up the reaction and drove the synthesis of bisethoxide forward for bulkier halides other than chlorine.

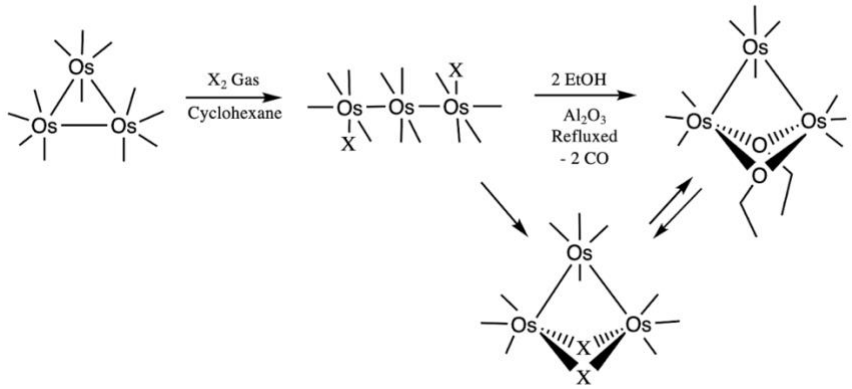

Figure D.4. Reaction mechanism of bridging halide complex with the addition of Alumina, Al_2O_3.

In 2016, Robert Sommerhalter conducted a systematic study with alumina in his initial reaction mixture to ensure the neutralization of the strong acid, with the goal of obtaining the best production of bisethoxide possible[27]. He tested each halide with each system – the linear $Os_3(CO)_{12}(X)_2$ and bridged $Os_3(CO)_{10}(\mu\text{-}X)_2$, in effort to see which produced the most effective yield of bisethoxide. From his results shown in Table D.1, chlorine remained the most successful halogen (75% net yield), as it consistently yielded bisethoxide from the linear $Os_3(CO)_{12}(Cl)_2$ and bridging $Os_3(CO)_{10}(\mu\text{-}Cl)_2$ routes, staying consistent with previous studies. Though chlorine showed the best overall results, a high net yield of bisethoxide (94%) from the bridging iodine complex $Os_3(CO)_{10}(\mu\text{-}I)_2$ showed potential in investigating iodine further. The obtained 94% yield from $Os_3(CO)_{10}(\mu\text{-}I)_2$,created a research question: how could we speed up the reaction of

the linear complex $Os_3(CO)_{12}(I)_2$ to effectively form the bridging halide intermediate $Os_3(CO)_{10}(\mu\text{-}I)_2$, to ultimately produce the best yield of bisethoxide quickly?

Table D.1. Results from Robert Sommerhalter's bisethoxide experiment, comparing the yields of bisethoxide obtained from differing halide intermediate routes performed[27].

$Os_3(CO)_{12}(X)_2$

X= halide	Yield of bisethoxide	Net yield from $Os_3(CO)_{12}$
Cl	79%	75%
Br	48%	none
I	25%	14%

$Os_3(CO)_{10}(X)_2$

X= halide	Yield of bisethoxide	Net yield from $Os_3(CO)_{12}$
Cl	57%	50%
Br	59%	none
I	94%	14%

In 2013, Powell published a paper that prepared bulky, heavy, osmium clusters rapidly by using a microwave to speed up the synthesis reaction time[17]. This research showed that the use of a microwave to assist the reaction sped up synthesis steps instead of hours of refluxing the solvent leading to a shorter reaction time, larger yield, and a route to more substituents. Because of these results, the Pearsall lab adopted this research mechanism to speed up the synthesis steps and aid in reaction yields, and the lab used it to produce bisethoxide in 2019[28].

The addition of the microwave to our synthesis steps allowed the Pearsall team to explore using iodine instead of chlorine further. Using the microwave led us to a way to speed up and promote the formation of the $Os_3(CO)_{10}(\mu\text{-}X)_2$ complex with 10 carbonyl ligands from the linear $Os_3(CO)_{12}(X)_2$ complex with 12 carbonyls. Currently, the Pearsall lab uses the synthetic approach shown in Figure D.5, which effectively yields high percentages of bisethoxide. This reaction mechanism utilizes the use of the microwave, and the use of the base alumina, discovered from past students' work.

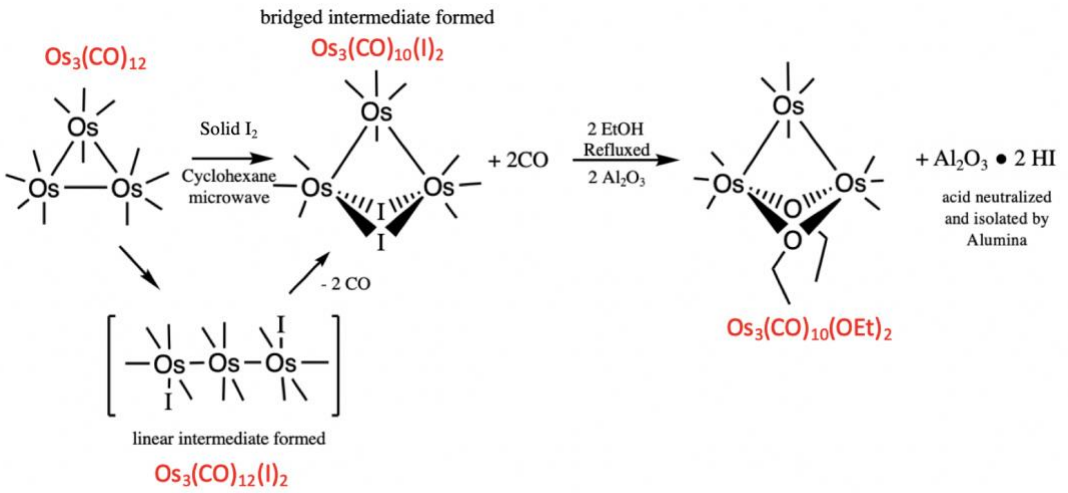

Figure D.5. Present Pearsall lab reaction synthesis steps to make our starting material, bisethoxide.

Sommerhalter's data (in 2016) did not yield presentable results for bromine, and so, the Pearsall lab would like to investigate why that occurred, re-examine and redo that reaction mechanism, and see if there is a route that would work to yield bisethoxide sufficiently from bromine. In the future, exploration of chlorine gas in a controlled quantity and reaction setting to see if it is possible to produce bisethoxide in good yield. Inspired by the CHEM 250L - Organic 1 Lab, Fall 2018 "Experiment #9: How can you halogenate an alkene? How do you assess the "greenness" of a chemical reaction?" where a green bromination reaction occurs using hydrobromic acid (HBr) and hydrogen peroxide (H_2O_2) to produce Br_2 gas and water (H_2O). On the basis of this, we want to create a green chlorination reaction using hydrochloric acid (HCl) and H_2O_2 to produce Cl_2 gas in a controlled environment (Figure D.6). In doing this, we would react the created chlorine gas with triosmium dodecacarbonyl ($Os_3(CO)_{12}$), to try to obtain bisethoxide faster, in higher yield, but in a less hazardous, "greener", reaction pathway in hopes of effectively yielding bisethoxide.

Organic Lab reaction:

$$HBr + H_2O_2 \rightarrow Br_{2\,(g)} + H_2O$$

Our reaction:

$$HCl + H_2O_2 \rightarrow Cl_{2\,(g)} + H_2O$$

$$Os_3(CO)_{12} + Cl_{2\,(g)} \rightarrow ?$$

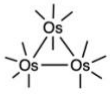

Figure D.6. Hypothesized green chlorination reaction, inspired by the Drew Organic 1 Lab.

On the basis of previous research done by Drew students in the Pearsall lab combined with literature, it has been shown that replacing one of the Os-Os bonds enhances the complex's reactivity. It has been shown that bisethoxide reacts in certain ways when reacted with different functional groups (Figure D.7)[29].

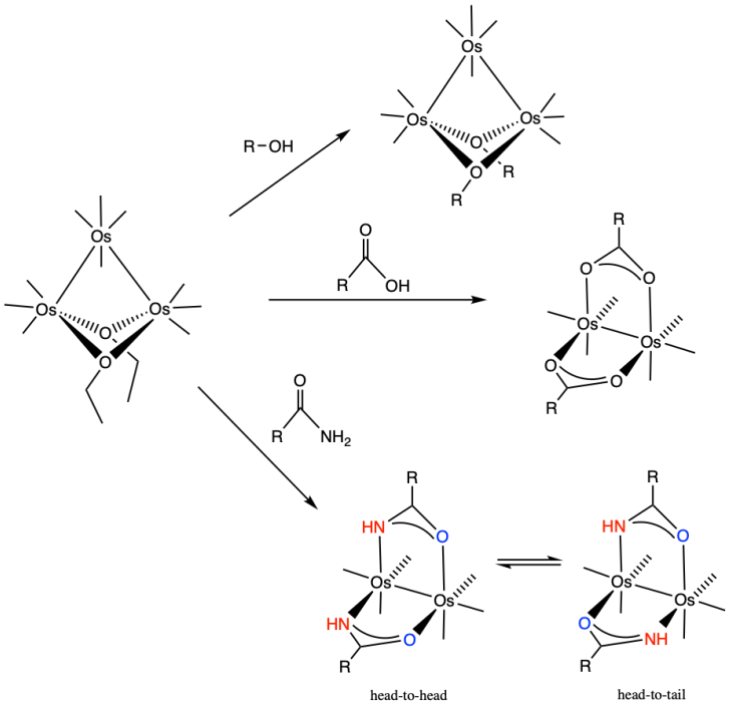

Figure D.7. Reactions with bisethoxide. Top structure is the product formed when bisethoxide is reacted with an alcohol. The middle product structure is when bisethoxide is reacted with a carboxylate. The bottom two product structures are the isomers that form when bisethoxide is reacted with an amide.

When bisethoxide reacts with an alcohol, the ethoxide ligand is replaced by that alcohol via substitution. When bisethoxide reacts with a carboxylate, it yields a diosmium complex with cis-bridging carboxylate ligands. This diosmium unit is also formed when bisethoxide is reacted with an amide, where the amide product forms two isomers: head-to-head and head-to-tail. Figure D.7 shows the two isomers; the head-to-head isomer has the nitrogens aligned on the same side, while the head-to-tail isomer has the nitrogens aligned on opposite sides. We can identify these structural changes by using IR spectroscopy to analyze the carbonyl ligand stretches. Knowing how bisethoxide reacts with various functional groups, in combination with known substitutional sites of bisethoxide, the possibilities of syntheses and experimental questions to answer are never ending.

8. Works Cited

(1) Kong, K. V.; Leong, W. K.; Ng, S. P.; Nguyen, T. H.; Lim, L. H. Osmium carbonyl clusters: a new class of apoptosis inducing agents. *ChemMedChem: Chemistry Enabling Drug Discovery* **2008**, *3* (8), 1269-1275.

(2) Morrison, E. C.; Leong, W. K.; Tan, J. Reduced overlap population analysis for triosmium clusters. *Journal of Cluster Science* **2007**, *18* (3), 753-763.

(3) Shojaie, A.; Atwood, J. D. Substitutional reactivity of dodecacarbonyltrimetal complexes of iron and osmium. *Organometallics* **1985**, *4* (1), 187-190.

(4) Pearsall, M.-A. Synthesis and reactivity of some osmium carbonyl clusters. University of Cambridge, 1984.

(5) Johnson, B. F. G.; Lewis, J.; Pippard, D. A. The preparation, characterisation, and some reactions of [Os3(CO)11-(NCMe)]. *Journal of the Chemical Society, Dalton Transactions* **1981**, (2), 407-412.

(6) Dunham, S. U.; Chifotides, H. T.; Mikulski, S.; Burr, A. E.; Dunbar, K. R. Covalent binding and interstrand cross-linking of duplex DNA by dirhodium (II, II) carboxylate compounds. *Biochemistry* **2005**, *44* (3), 996-1003.

(7) Kong, K. V.; Leong, W. K.; Lim, L. H. Induction of apoptosis by hexaosmium carbonyl clusters. *Journal of Organometallic Chemistry* **2009**, *694* (6), 834-839.

(8) Kong, K. V.; Leong, W. K.; Lim, L. H. K. Osmium Carbonyl Clusters Containing Labile Ligands Hyperstabilize Microtubules. *Chemical Research in Toxicology* **2009**, *22* (6), 1116-1122.

(9) Lee, H. Z.; Leong, W. K.; Top, S.; Vessières, A. Cytotoxic triosmium carbonyl clusters: a structure-activity relationship study. *ChemMedChem* **2014**, *9* (7), 1453-1457.

(10) Kwek, Z. H.; Ganguly, R.; Afreen, A. M.; Koh, W. X.; Leong, W. K.; Tan, Y. L. K. Carboxylated Chalcone and Benzaldehyde Derivatives of Triosmium Carbonyl Clusters: Synthesis, Characterization and Biological Activity Towards MCF-7 Cells. *Journal of Cluster Science* **2020**, *31* (4), 759-767.

(11) Elias, D.; Beazely, M.; Kandepu, N. Bioactivities of chalcones. *Current medicinal chemistry* **1999**, *6* (12), 1125.

(12) Lee, J. J. Y.; Leong, W. K. Towards understanding the mode of action of the cytotoxic triosmium carbonyl cluster Os3 (CO) 10 (NCCH3) 2: Its reactivity with amino acids and oligopeptides. *Journal of Organometallic Chemistry* **2020**, *924*, 121459.

(13) Marino, S. M.; Gladyshev, V. N. Analysis and functional prediction of reactive cysteine residues. *Journal of Biological Chemistry* **2012**, *287* (7), 4419-4425.

(14) Dunham, S. U.; Remaley, T. S.; Moore, B. S.; Evans, D. L.; Dunham, S. U. Isolation, Characterization, and DNA Binding Kinetics of Three Dirhodium (II, II) Carboxyamidate Complexes: Rh2 (μ-L)(HNOCCF3) 3 where L=[OOCCH3]−,[OOCCF3]−, or [HNOCCF3]−. *Inorganic Chemistry* **2011**, *50* (8), 3458-3463.

(15) Deans, A. J.; West, S. C. DNA interstrand crosslink repair and cancer. *Nature Reviews Cancer* **2011**, *11* (7), 467-480. DOI: 10.1038/nrc3088 (acccessed 2022-04-28T01:34:32).

(16) Unpublished research. Infrared Spectrum of Os3CO10 in CH2Cl2. University., D., Ed.; Pearsall Research Resources Moodle Site. Unpublished results. Infrared Spectrum of Os3(CO)10(OEt)2. Drew University: Pearsall Research Resource Moodle Site.

(17) Pyper, K. J.; Kempe, D. K.; Jung, J. Y.; Loh, L.-H. J.; Gwini, N.; Lang, B. D.; Newton, B. S.; Sims, J. M.; Nesterov, V. N.; Powell, G. L. Microwave promoted oxidative addition reactions of Os3 (CO) 12: efficient syntheses of triosmium clusters of the type Os3 (μ-X) 2 (CO) 10 and Os3 (μ-H)(μ-OR)(CO) 10. *Journal of Cluster Science* **2013**, *24* (3), 619-634.

(18) Higgins, S. Unpublished Work. Infrared Spectrum of Os3(CO)9(OEt)2(MeCN) in CH2Cl2. Measured in Transmittance. Drew University: Pearsall Research Resource Moodle Page, 1997.

(19) Higgins, S. Unpublished work. Infrared spectra of Os3(CO)9(OEt)2(P(OMe)3) and Os3(CO)8(OEt)2(P(OMe)3)2 in CH2Cl2. Measured in transmittance. Drew University: Pearsall Research Resource Moodle Page, 1997.

(20) Moore, D. Reactions of Triosmium Carbonyl Clusters: Phosphine Substitution Reactions and the Reactivity of Os3(CO)10(OH)2 and Os3(CO)9(OH)2(P(OMe)3). Honors Thesis. Drew University: Madison, NJ, 1998.

(21) Johnson, B.; Lewis, J.; Kilty, P. Chemistry of polynuclear compounds. Part XIII. The preparation and some reactions of dodecacarbonyltriosmium. *Journal of the Chemical Society A: Inorganic, Physical, Theoretical* **1968**, 2859-2864.

(22) Schlecht, S. Unpublished Results. Drew University: Madison, NJ., 1996.

(23) Shah, A. Unpublished Results. Pearsall Lab. Drew University: Madison, NJ, 2010.

(24) Shah, A. Unpublished Results. Drew University: Madison, NJ, 2010.

(25) Portero, E. Unpublished Results. Drew University Summer DSSI. Madison, NJ, 2012.

(26) Portero, E. Organometallic Chemistry: Synthetic approaches to linked Carboxylate Osmium Carbonyl Clusters. Reactions of Os3(CO)10(μ2-OEt)2 with 1,10-decanedicarboxylic acid. Unpublished Results. Drew University: Madison, NJ, 2015.

(27) Sommerhalter, R. E. New Synthetic Approaches to Triosmium Decacarbonyl Bisethoxide and the Systematic Design of Linked Triosmium Clusters Via Bridging Diols. Drew University, 2016.

(28) Costa, S. Honors Thesis. Reactivity of Os2(CO)6(RCONH)2: mechanisms and thermodynamic properties. Drew University: Madison, NJ, 2019.

(29) Marak, K. E. Some Reactions of Triosmium Decacarbonyl Bisethoxide, Os3 (CO) 10 (μ2-OEt) 2, with Amides. Drew University, 2017.